

## **Positronium Atom in Solids – Peculiarities of Formation and Interconnection with Free Volume Nanostructure –**

**V. P. Shantarovich\***

*N.N. Semenov Institute of Chemical Physics, Russian Academy of Sciences, Kosygin st. 4, 119991 Moscow, Russia*

*Received: March 10, 2006*

The recent several decades have seen the spectacular advances in a new area at the junction of elementary particle physics and chemistry, the so called chemistry of new atoms in which either electron is replaced by another negative particle or a proton by another positive particle. The area of research does not confine itself to chemical studies alone. External influences on the properties of new atoms provide useful, sometimes unique information about the structure of solids. In this review, we survey briefly properties of the new atoms and illustrate the last statement on example of positronium, the simplest hydrogen-like atom, where pick-off annihilation process gives valuable information on the free volume nanostructure of solids.

### **1. Introduction to new atoms**

One feature of the vehement growth of physics in the 20th century is, undoubtedly, the correlation of this science with other fields of human endeavor, their mutual enrichment. The recent several decades have seen the spectacular advances, for example, in a new area at the junction of elementary-particle physics and chemistry, the so-called chemistry of new atoms, in which either an electron is replaced by another negative particle or a proton by another positive particle. This area of research does not confine itself to chemical studies alone. External influences on the properties of new atoms, and also those of mesons and positrons, provide useful, sometimes unique, information about the structure of solids. Therefore, unlike other reviews on positron annihilation, this paper includes a special part, describing intrinsic properties of positronium in comparison with properties and composition of other new atoms, so that this part can be considered as a general introduction into the field of new atoms. On example of positronium, the main part of this paper demonstrates external influences of the surrounding matter on properties and characteristics of one of the new atoms and the use of this effect for structural studies in solids. Correspondingly, a newcomer will find in this paper a little more than one of the special applications of the positron annihilation method.

Atoms with an electron replaced by a negative meson are called mesoatoms. When chemically bound to conventional molecules and radicals they form mesomolecules. Typical examples are  $\mu^-$ - and  $\pi^-$ -mesoatoms.

Also possible in principle are E-mesoatoms, in which an electron is replaced by a negative hyperon, antiproton, or antihyperon.

Atoms with a proton replaced by a positive particle are called by the name of that particle with an ending 'ium'. Since a penetration of any positive particle into a nucleus is hindered by Coulomb repulsion (which can be compensated for by the nuclear forces alone), for light positive particles not involved in nuclear interactions, such as positrons  $e^+$  and  $\mu^+$ -mesons, the atoms of this type cannot have nuclei consisting of many nucleons. These atoms only form when a positive lepton replaces a single nucleon, namely, a proton. In that case, an atom of a positron and an electron is called positronium (Ps). A bound system of  $\mu^+$ -meson (positive muon) and an electron is known as muonium (Mu). Both atoms can be treated as light isotopes of hydrogen.

What is more, positronium is the lightest of all known new atoms, the only atom without a nucleus. In fact, since both constituent particles have the same mass, the centre of mass does not coincide with any of them (otherwise such a particle could be regarded as a nucleus), but lies strictly in between them.

A nuclear proton can also be replaced by a positively charged hyperon in much the same way as a neutron by a neutral hyperon. The result is the so-called hypernuclei, and the corresponding atoms are referred to as hyperatoms. The structure of their electron shells and their chemical properties are, however, essentially the same as in conventional atoms with the same nuclear charge. Therefore, hyperatoms are generally not included into the list of new atoms.

Interest in new atoms chiefly comes from the fact that their characteristics are appreciably influenced by the chemical properties and the structure of their environment. We will be looking at them in more detail in the next section. Examination of the characteristics of new atoms can supply unique evidence concerning the properties of the environment. One important characteristic of new atoms is their lifetime (all of them unstable). The decay characteristics of new atoms are studied using the apparatus of nuclear physics.

The first stage of new atom research is the study of the laws by which the environment affects the characteristics and fate of new atoms. The second stage, more important for other research fields, consists in obtaining more complete and new structural and chemical data or data on the kinetics of certain processes based on observations of characteristics of formation, transformation, and disintegration of various new atoms.

At the present time both the investigations into annihilation (death) of positrons and positronium and the mesochemical studies of  $\mu^-$ - and  $\pi^-$ -mesoatoms and muonium have attained the second stage and started to yield information of general chemical significance. The field is very extensively promising. The aim of this review is not to embrace the whole problem of "new atoms" or the most of directions of positron annihilation studies. Instead, after general introduction into physics and methodology, detailed discussion is given of so called positronium pick-off annihilation and application of this effect for the studies of the free volume nanostructure in solids, in polymers particularly.

### **2. Composition and properties of positronium and other new atoms.**

Table 1 is a summary of some of the properties of elementary particles constituting the new atoms. Particle masses are

\*Corresponding author. E-mail: Shant@chph.ras.ru

**TABLE 1: Some properties of the elementary particles of which new atoms are made up**

Name	Symbol	$m$ , rel. units	$m$ , MeV/ $c^2$	Charge	Lifetime, s
Electron	$e^-$	1	0.511	-1	Stable
Positron	$e^+$	1	0.511	+1	Stable
$\mu$ -meson	$\mu^\pm$	206.77	105.66	$\pm 1$	$2.26 \times 10^{-6}$
$\pi$ -meson	$\pi^\pm$	273.15	139.58	$\pm 1$	$2.56 \times 10^{-8}$
Proton	p	1836.1	938.2	+1	Stable

**TABLE 2: Properties of hydrogen-like atoms**

Name	Symbol	Composition	$\mu$	$r$ , cm	$V_{ion}$ , eV
Hydrogen	H	$pe^-$	1	$0.529 \times 10^{-8}$	13.595
Positronium	Ps	$e^+e^-$	$1/2$	$1.05 \times 10^{-8}$	6.80
Muonium	Mu	$\mu^+e^-$	0.995	$0.532 \times 10^{-8}$	13.539
$\mu$ -Mesohydrogen	-	$p\mu^-$	185.8	$2.85 \times 10^{-11}$	-
$\pi$ -Mesohydrogen	-	$p\pi^-$	237.8	$2.23 \times 10^{-11}$	-

given in relative (in relation to the electron mass) units and in "energy" units that correspond to Einstein equation. Unstable mesons decay in the following way:

$$\mu^\pm \rightarrow e^\pm + \nu_e(\bar{\nu}_e) + \bar{\nu}_\mu(\nu_\mu) \quad (1)$$

$$\pi^\pm \rightarrow \mu^\pm + \nu_\mu(\bar{\nu}_\mu) \quad (2)$$

where  $\nu$  and  $\bar{\nu}$  are the corresponding neutrino and antineutrino. The positron as such is a stable particle and it only disappears as a result of its interaction with the environment. In the previous section we have already mentioned that positronium and muonium are hydrogen-like. Replacement of the electron in the hydrogen atom by  $\pi^-$  or  $\mu^-$  meson yields mesohydrogen. Characteristics of hydrogen-like new atoms are given in Table 2. The reduced mass – a parameter that is fairly important for determining other characteristics of new atoms – is calculated from the given masses of the constituent particles  $m_1$  and  $m_2$ :  $\mu = m_1 m_2 / (m_1 + m_2)$ .

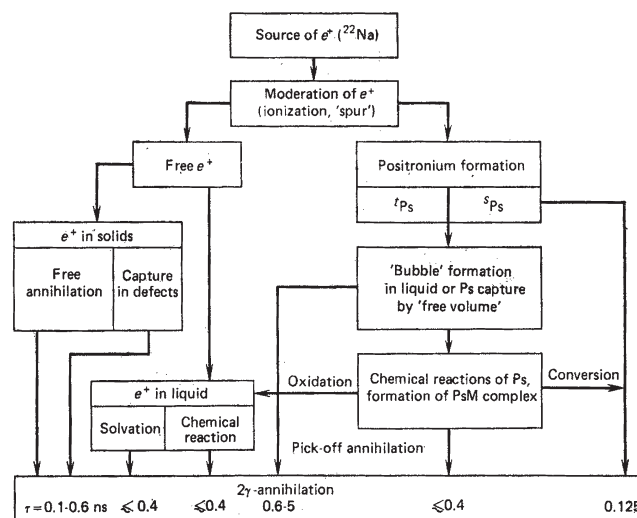
In terms of reduced masses positronium has only half the mass of the atomic hydrogen, while in terms of absolute masses the latter is 920 times heavier. Because of the difference in reduced masses the ionization potential  $V_{ion}$  (i.e. the binding energy) of positronium is half of that for the hydrogen atom, and the distance  $r$  between the electron and the positron is twice that between the proton and the electron (twice the Bohr radius). Although positronium consists of stable particles (the electron and positron are particle and antiparticle), they can kill each other (annihilate) and give off  $\gamma$ -quanta. This process is responsible for the instability of the positronium, and for its extremely short lifetimes ( $\sim 10^{-7}$  and  $10^{-10}$  s in a vacuum).

Although muonium and atomic hydrogen differ markedly in mass, their reduced masses and hence some other characteristics are similar.

The main feature of mesohydrogen is that the radius of the meson orbit is about 1/200 of the Bohr radius. Therefore, the positive charge of the proton is highly screened and in many respects mesohydrogen behaves as a neutral particle similar to neutron.

### 3. Positron annihilation studies

At present the bibliography of this expanding area of research<sup>1</sup> includes more than 2000 publications. The details of the theories and experimental techniques are discussed in books<sup>2-6</sup> and in a number of review articles,<sup>7-15</sup> including those devoted to the general overview of new atoms.<sup>10,13</sup> Recently the 13th and 14th International Conferences on Positron Annihilation (ICPA13, 14) and 8th International Workshop on Positron and Positronium Chemistry PPC-8 were held.<sup>16,17</sup> Experimental data are summarized in review tables.<sup>18,19</sup>

**Figure 1.** Scheme of positron annihilation processes

This review does not claim to be a profound analyses of the current work. Its objective is to give a general idea of positron annihilation research and application of these investigations mostly in the free volume studies. In some way, this review continues a discussion of the possibilities of positron annihilation experiments, started several years ago by publication in this journal<sup>20</sup> and in the other Journal.<sup>21</sup>

**3.1. Annihilation and interaction of positrons with matter.** As a positron and an electron interact, their kinetic energies and rest masses transform into  $\gamma$ -quanta. This process is called annihilation and is governed by general physical laws of conservation (of energy, momentum, parity, etc.).

By the law of parity conservation in annihilation two or three  $\gamma$ -quanta are produced depending on the relative orientation of the spins of the electron and the positron (for parallel spins three quanta, and for antiparallel spins two quanta).

In the case of a two-photon annihilation of an electron-positron pair at rest the  $\gamma$ -quanta fly off in strictly opposite directions (at  $180^\circ$ ) in accordance with the law of momentum conservation. The energy of each quantum is equivalent to the electron rest mass (0.511 MeV). Slight deviations from 0.511 MeV of the photon energies or from collinearity of the emission directions give valuable information about the properties of matter and are the core of a number of experimental techniques.

The fate of energetic positrons emitted by radioactive sources (e.g.  $^{22}\text{Na}$ ) is annihilation. But before this really happens some processes may occur, which are shown in Figure 1. In a condensed phase positrons are slowed down in only several picoseconds (mainly by ionization and excitation of surrounding molecules).

**TABLE 3: Properties of the positronium atom**

Property	Type of state	
	Singlet ( <i>p</i> -Ps)	Triplet ( <i>o</i> -Ps)
Symbol	<sup>s</sup> Ps	<sup>t</sup> Ps
Spin state	e↑↓e <sup>+</sup>	e↑↑e <sup>+</sup>
Quantum number	<i>J</i> =0	<i>J</i> =1
Share, %	25	75
Proper lifetime, s	1.25×10 <sup>-10</sup>	1.4×10 <sup>-7</sup>
Annihilation type	2γ	3γ

A fraction of positrons undergo free annihilation with surrounding electrons. In liquids this process may be preceded by solvation. Some positrons may get involved in chemical reactions and further annihilate from the bound state Me<sup>+</sup> with a molecule or ion M. In the case of free annihilation a two-photon event is 372 times more probable than a three-photon event. And for the free annihilation of positrons the lifetime is about 0.4 ns.

The remaining positrons form a bound positron-electron systems called positronium (Ps). Depending on the relative alignment of spins of the electron and the positron, positronium can have two states: singlet and triplet. The properties of the positronium atoms are tabulated in Table 3. It is seen that the proper lifetime (in a vacuum) of a triplet positronium (3γ-annihilation) is three orders of magnitude longer than for a singlet positronium. But a variety of interactions shown in Figure 1 shorten the lifetime of positronium in a condensed phase down to several nanoseconds. In positronium-forming systems the free annihilation of some of triplet positronium increases the share of 3γ-annihilation as compared with the case of free annihilation of positrons.

Measurements of lifetimes of triplet positronium and the angular distribution of the annihilation radiation of singlet and triplet positronium, as well as Doppler broadening of annihilation line, provide an insight into positronium reactions and the chemical properties of the environment. These studies are the main part of positronium chemistry.

**3.2. Positronium formation.** As is seen in Figure 1, not all positrons (and not in all substances) form positronium. Experimentally, this share can be estimated, for example, by measuring the intensity of the positronium-related long-lived component. Now there are two views of the process of positronium formation, although their combination seems to give the most complete picture of the phenomenon.

By the model of the Swedish physicist Ore<sup>22</sup> positronium can form within a narrow energy interval between the ionization potential of the surrounding molecules, *V*<sub>ion</sub> and (*V*<sub>ion</sub>–6.8) eV, where 6.8 eV is the binding energy for positronium (half a rydberg). If we take into account the excitation of the first electron level *E*<sub>1</sub> of surrounding molecules, a process that competes with positronium formation, the interval will become narrower; and eventually for a positron that effectively forms a positronium, the energy interval will be *E*<sub>1</sub><*E*<sub>e<sup>+</sup></sub><*V*<sub>ion</sub>–6.8, and the proportion of positrons that form positronium, *P*, will be given by eq 3:

$$\frac{6.8}{V_{\text{ion}}} < P < \frac{E_1 - (V_{\text{ion}} - 6.8)}{E_1} \quad (3)$$

Positronium here can have a kinetic energy from zero to *V*<sub>ion</sub> or to *E*<sub>1</sub>. It seems obvious now that the model only gives a correct prediction of positronium formation in inert gases though some attempts were made to use the same considerations in liquids<sup>23,24</sup> and participation of unthermalized positrons in positronium formation can not be ruled out.

Another, so-called spur, model was first suggested by Mogensen<sup>25</sup> and developed by other authors<sup>26-29</sup> as a diffusion-

recombination model. This model better explains the evidence for positronium formation in liquids. The underlying idea of the spur model is the assumption that positronium forms when a positron at the end of its moderation combines with one of the electrons of its own spur or, more exactly, with one of the “blob” electrons. By “blob” is here meant the unstable cluster of electrons, positive ions and radicals that emerge as a positron is moderated in a liquids and perhaps in some solids.<sup>30-33</sup>

The probability of positronium formation in the positron spur depends mainly on the rates of the competing processes. In the general form the process can be represented as follows:



In pure solvent, obviously, only reactions (4) and (5) should be considered. In the presence of active impurities *S*<sub>1</sub>, *S*<sub>2</sub>, *S*<sub>3</sub> the processes (6)–(8) also play a part. They lead either to inhibition or an increase in the percentage of positrons that form positronium. The rates of the processes (5)–(7), and hence the probability of positronium formation, are quite sensitive to the physico-chemical properties of the environment and they are measured in radiation chemistry. No wonder, therefore, that a number of interesting correlations have been found between positronium chemistry and radiation chemistry.<sup>34-40</sup> Much work is being done currently in this direction to study the details of the spur mechanism.<sup>41-43</sup> A new technique of single-photon count with radioactive (including positron) sources has appeared, which allowed observations of the correlation of inhibition of the recombination fluorescence intensity and positronium formation by the same acceptors.<sup>44</sup> Recently, similar behavior was observed for low-temperature positronium formation and thermo-stimulated luminescence (TSL) in some polymers.<sup>45</sup> The presence of these correlations is evidence of the predominance of spur processes in positronium formation not only in liquids but also in solids. We have to stress however that in solids positronium observations are influenced also by the presence and characteristics of the so-called free or unoccupied volume.<sup>46,47</sup>

**3.3. Positron annihilation experiments.** Information about the fate of positrons and positronium and about the properties of their environment can be obtained from examining the characteristics of the annihilation radiation emitted in positron decay. Each of the techniques available is aimed at investigating certain characteristics:

(1) The number of γ-quanta emitted in annihilation. The corresponding method of double or triple coincidences is the least informative.

(2) The angular distribution of annihilation radiation. Here information is derived about the momentum distribution of electrons involved in annihilations. If positrons or positronium take part in chemical reactions, the shape of the distribution changes.

(3) The energy spectrum of annihilation γ-quanta (deviation from 0.511 MeV registered using a Ge(Li)-semiconductor detector of the Doppler broadening) also represents the energy distribution of electrons involved in annihilation. Especially informative is a work with the coincidences of signals from the two Doppler broadening detectors (CDB technique), where this method becomes sensitive to positron annihilation on the core electrons of different elements.

(4) The time distribution of annihilation radiation. It is strongly dependent on electron density at the location of a positron or positronium and on the rate at which positronium enters into chemical reactions.

Various radioactive isotopes can be used as positron sources. Of these <sup>22</sup>Na is the commonest both due to its rather long half-

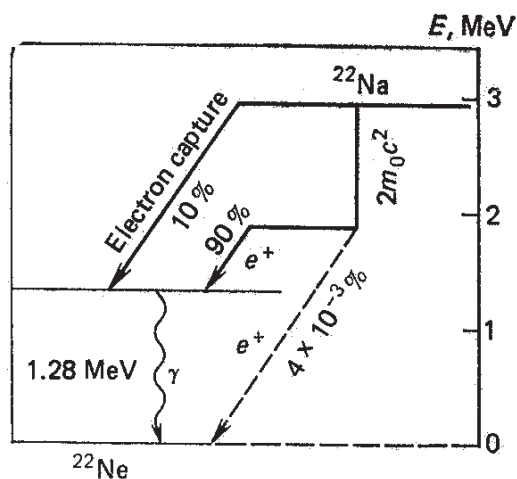


Figure 2. The decay scheme of the positron-active  $^{22}\text{Na}$ .

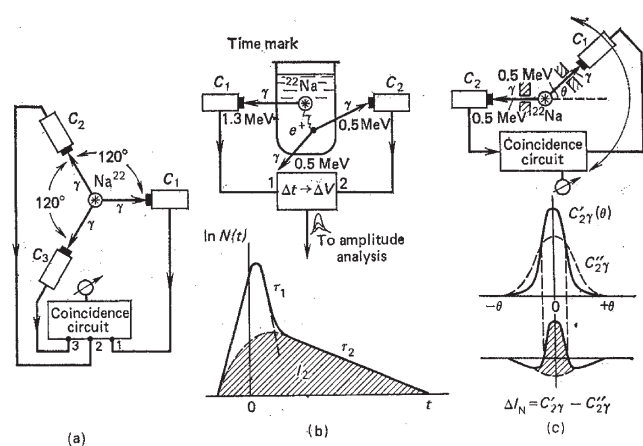


Figure 3. Experimental arrangements: (a) triple coincidence circuit, (b) observation of lifetime distribution of positron annihilation, (c) measurements of angular correlation of positron annihilation.

life (2.58 years) and to its applicability in various experimental arrangements. The decay scheme for  $^{22}\text{Na}$  is shown in Figure 2. Depending on the technique used, sources can have different activities which vary from tens of  $\mu\text{Ci}$  for positron lifetime measurements and studies of the Doppler broadening of the annihilation line to a hundred  $\text{mCi}$  in angular correlation measurements. In the first case activities are limited by the growth of the random coincidence background. A source is prepared by evaporating a drop of  $^{22}\text{NaCl}$  radioactive solution on a thin (1–2  $\text{mg}/\text{cm}^2$ ) metal foil or synthetic film that pass positrons well, the source is then covered with the same material (foil or film). When working with liquids it is also convenient to use sources prepared by diffusing at an elevated temperature of  $^{22}\text{NaCl}$  into 2–4  $\text{mg}/\text{cm}^2$  glass foil.<sup>48</sup> Another positron source can be a positron beam of certain energy produced at accelerators.<sup>49</sup> The last technique is commonly used in studies of the chemical state and physical properties of surfaces of solid specimens, and also in studies of the depth distribution of defects.

The common experimental arrangements are depicted in Figure 3. Shown in Figure 3a is the triple coincidence arrangement to record *ortho*-positronium (*o*-Ps) annihilation events with the emission of three  $\gamma$ -quanta. They are recorded by counters  $C_1$ ,  $C_2$ , and  $C_3$ . The technique has the disadvantage that the counting rate for triple  $\gamma$ -coincidences ( $C_{3\gamma}$ ) is proportional to the product of two variables — the percentage of positrons,  $P$ , that form positronium and the probability of an annihilation with the ejection of three  $\gamma$ -quanta  $W_{3\gamma} = \tau_3/\tau_T^0$  ( $\tau_3$  is the real lifetime of positronium in matter, and  $\tau_T^0$  is the lifetime of triple positronium in a vacuum (see Table 3)). Therefore,  $C_{3\gamma}$  can go

down both because of shorter positronium lifetime (smaller  $W_{3\gamma}$ ) and because of positronium formation inhibition (smaller  $P$ ). It is desirable, however, to distinguish the contributions of these two interactions.

The most variegated information is supplied by observations of the time spectrum of positron annihilation (see Figure 3b) using coincidence circuits that record delayed coincidences  $N(t)$  between a nuclear  $\gamma$ -quantum with energy 1.3 MeV (counter  $C_1$ ) emitted essentially simultaneously with the ejection of a positron from a  $^{22}\text{Na}$  nucleus, and a 0.5 MeV  $\gamma$ -quantum (counter  $C_2$ ) produced by a  $2\gamma$ -annihilation of that positron. Thus, the times of creation and decay of that positron are recorded. The short-lived components of the time spectrum (lifetimes  $\tau_1$ ,  $\tau_2$  with intensities  $I_1$ ,  $I_2$ ) are due to the annihilation of positrons in *para*-positronium ( $^s\text{Ps}$ , see Table 3) and in free collisions with electrons; whereas the long lived component (lifetime  $\tau_3$ , intensity  $I_3 = 3/4P$ ) is due to the annihilation of the positrons that have formed triplet positronium. The time resolution (the width of the prompt coincidence curve at half maxima FWHM) for present-day apparatus is about 0.2–0.3 ns.

This technique distinctly distinguishes positronium quenching and positronium formation inhibition. In the simplest case of pure inhibition the intensity  $I_3$  of the long-lived component decreases without decreasing the slope of the “tail” of this component that characterizes its lifetime  $\tau_3$ . But with pure quenching,  $\tau_3$  decreases while  $I_3$  remains unchanged. In positron annihilation experiments we will encounter examples of changes in time spectra of annihilation due to inhibition and quenching. Strictly speaking, when the lifetime of positronium in a solution becomes shorter (quenching) due to the use of active additives, kinetic equations<sup>50</sup> determine the relation (see eq 9) between the percentage of positrons  $P$  that form positronium in the solution and the observed intensity of the long-lived component  $I_3$ :

$$I_3 = (3P/4)(\lambda_B - \lambda_P)/\{(\lambda_B - \lambda_P) - k[\text{Ac}]\}, \quad (9)$$

where  $\lambda_P$  is the rate of annihilation at solvent molecules, the so-called *pick-off* annihilation;  $\lambda_B$  is the rate of annihilation of positronium in bound state with active additive ( $\lambda_B = 1/\tau_B$ ,  $\tau_B \leq 0.4$  ns, see Figure 1);  $k[\text{Ac}]$  is the positronium quenching rate.

The single-photon count technique with positron sources,<sup>44</sup> mentioned in sec. 3.2, was in fact a modification of apparatus designed to study positron lifetimes in which the annihilation  $\gamma$ -quantum detector is replaced by a single-photon one.

Figure 3c represents a third major technique — the observation of correlation curves, i.e. dependences of coincidence counting rate of two annihilation  $\gamma$ -quanta ( $C_{2\gamma}$ ) with energy 0.5 MeV ( $C_1$  and  $C_2$ ) on the angle  $\theta$ , i.e. on the deviation from  $180^\circ$  of the angle between two ejected quanta. The detectors are located at about 2 m from the sample behind lead collimators. Differentiating  $dC_{2\gamma}/d\theta$  gives the momentum distribution function for electrons in matter  $\rho(P_Z)$ . The narrowest component of the complicated correlation curve corresponds to singlet positronium annihilation. Therefore, by separating in a large experimental run the correlation curves shown schematically in Figure 3c into the narrow  $I_N$  and wide components we can obtain important additional information about positronium chemical reactions, namely we can distinguish the various positronium quenching forms. Actually, the annihilation of *o*-Ps on “foreign” electrons in collisions, just as the formation of chemical compounds  $\text{PsM}$  in substitution and addition reactions, and the annihilation of *o*-Ps oxidation products — free positrons — yield correlation curves several milliradians wide. Special approaches were suggested to distinguish and identify both the case of addition and the case of oxidation.<sup>51,52</sup> Positronium conversion from a triplet state into a singlet one with subsequent  $2\gamma$ -annihilation increases in the correlation curve the intensity of the narrow component and can also be

easily identified.

The coming of Ge (Li)-semiconductor detectors (SD) with high energy resolutions (1 keV at the energies about 500 keV) opened up new possibilities to do without angle correlation set up. In fact, if  $X$  is the direction from a positron source to a detector, then since  $\Delta E_\gamma = P_X c/2$ , the electron energy  $E$  (positron is assumed to be at rest), the momentum component  $P_X$  and the annihilation line broadening  $\Delta E_\gamma$  will be related by eq 10:

$$E = P_X^2 / 2m_e = 2(\Delta E_\gamma)^2 / m_e c^2. \quad (10)$$

Thus, the Doppler shift of a  $\gamma$ -quantum by 1 keV, i.e. only by 0.2%, corresponds to an electron energy of 3.9 eV. Since under experimental conditions

$$\sin\theta = P_Z / m_e c \cong \theta \quad (11)$$

( $Z$  is the direction normal to the plane passing through the collimator slit of the stationary detector and through the sample — see Figure 3c), then in isotropic case

$$\theta = 2\Delta E_\gamma / m_e c^2 \quad (12)$$

Here a 1-keV broadening is equivalent to a deviation of 3.9 mrad from collinearity in quantum ejection. In other words, a detector with a high (in modern terms) energy resolution is equivalent to an angular installation with a resolution of about 4 mrad, a resolution four times worse than in a conventional angular experiment. Nevertheless special computer programs take into account resolution functions and make it possible to extract the information required.<sup>53</sup> It was mentioned already, that a set up with coincidence of the two detectors (CDB technique) essentially diminishes a background and gives an elemental sensitive instruments for solid state structure studies and for identification of the mechanisms of the positron trapping.<sup>54-56</sup>

**3.4. Positronium quenching.** The lifetime of *o*-Ps in normal liquids and solids (0.6–5 ns) appears to be much shorter than its proper lifetime (140 ns, see Table 3). This is due to pick-off annihilation, i.e. the annihilation of positronium's positron on electrons of surrounding molecules. The lifetime of positronium becomes yet more shorter in the presence of small amounts of positronium-active molecules (quenchers). Positronium is quenched through its chemical transformations. They were discussed previously.<sup>6,20,21</sup> Here, we will look at pick-off annihilation.

*Pick-off annihilation. Bubble formation. "Free volume" model.* This subsection is concerned with two main hypotheses of the pick-off annihilation of positronium. For liquids this is the so-called bubble model which has first been formulated for condensed gases;<sup>57-59</sup> it is also of importance for an understanding of the mechanism of positronium chemical reactions in liquids.<sup>60-69</sup> For solids, e.g. polymers, the "free volume" model is suggested in Reference 70.

The bubble model assumes that in the majority of liquids around positronium a bubble is formed. This model approximates the bubble around a Ps atom as a square well with spherical geometry. This potential well has a radius  $R$  a depth  $U$  and the energy of positronium  $E$ , measured from the bottom of the well. According to References 57–59, the bubble radius is determined by minimizing with respect to  $R$  the total energy of the bubble  $E_{\text{tot}} = E_{\text{cm}}(R, U) + (4/3)\pi R^3 P + \sigma 4\pi R^2$ , where  $E_{\text{cm}}$  is the zero point energy of the trapped positronium, the second term is the pressure-volume work, and the last term is the surface energy due to the bubble-fluid interface with specific surface energy  $\sigma$ . The minimization of  $E_{\text{tot}}$  gives eq 13:

$$\frac{\sin^4(kR)}{kR(\tan(kR) - kR)} = -\frac{\pi \hbar^2 \gamma}{m_e U^2}, \quad (13)$$

where  $k = (4m_e E/2)^{1/2}$ , and  $m_e$  is the mass of an electron. Existence of the solution of eq 13 is a condition of the bubble formation.<sup>60</sup>

The specific rate of pick-off annihilation is given by eq 14:

$$\lambda_p / N = \pi r_0^2 c n Z_{\text{eff}} P(kR) = \pi r_0^2 c N_A \frac{Z_{\text{eff}}}{V} P(kR), \quad (14)$$

where  $P(kR) = \sin^2(kR)[1 - kR \times \cot(kR)]^{-1}$  and expresses the quantum mechanical probability for Ps atom coming out of the well;  $r_0$  is classical radius of an electron,  $c$  is the velocity of light,  $n$  is the number of molecules in unit volume,  $N_A$  is Avogadro's number and  $V$  is the molecular volume,  $Z_{\text{eff}}$  is the effective number of annihilating electrons per molecule, which was proved to be equal to the number of valence electrons per molecule.<sup>57-59</sup> Experimental lifetimes ( $\tau_p = \lambda_p^{-1}$ ) in majority of liquids give the following bubble parameters:  $R = 3-4.5 \text{ \AA}$ ,  $U \approx 1 \text{ eV}$ .

Growth and shrinking of the positronium bubble influence the rate of positronium pick-off annihilation and chemical reactions. In the work,<sup>71</sup> the effect of the bubble on chemical reaction is seen from the good correlation of the *o*-Ps quenching rate with surface tension of various solvents and with energy of the system "Ps in a bubble". Obviously, bubble formation influences PsAc complex formation and the complex decomposition. We touched here the idea of the positronium bubble formation since this peculiarity of Ps interaction with a substance may be important for positronium annihilation in elastic polymers at high temperatures. The role of this effect must be found from comparison of the rate of the bubble growth and the rate of positronium annihilation, as it was done for a number of liquids in paper.<sup>72</sup> It was shown that in such viscous liquids as glycerol the bubble has no time to reach equilibrium size before *o*-Ps annihilation. Experiments<sup>73</sup> show that one of the signs of equilibrium bubble formation can be found in appearing of additional intermediate momentum component in the ratio curves of CDB spectra of liquids relative to those in their solid state for *n*-hexane and cyclohexane (Figure 4). In contrast, such components were not found at low temperatures in some liquids with low freezing points and in rubbery polymers

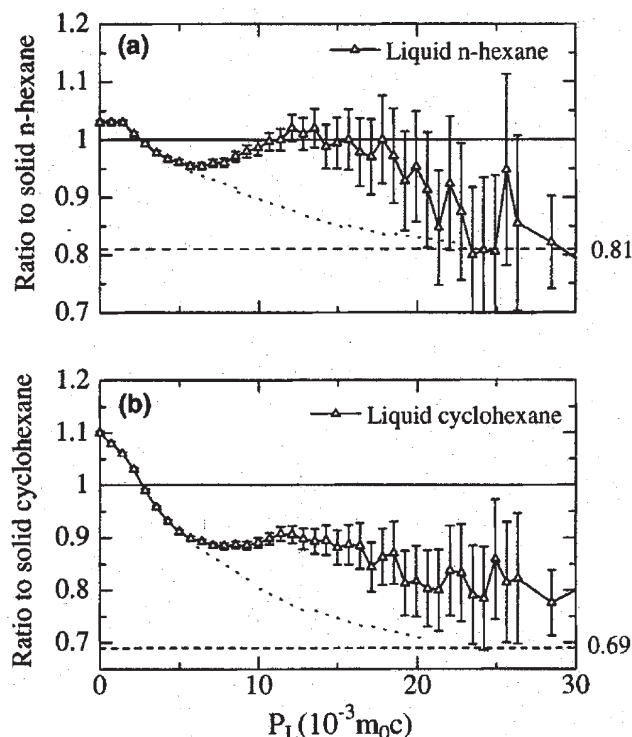


**Figure 4.** Ratio curves of CDB spectra for *n*-hexane (a), and cyclohexane (b) in liquid state relative to their solid state. The dashed lines as well as the values shown at the right side of each graph illustrate the expected level or ratios due to  $I_3$  difference. The dotted lines demonstrate the expected variation tendency of the ratio curves due to  $I_3$  difference.<sup>73</sup>

(above  $T_g$ ), which may show absence of equilibrium bubble in these cases. Detailed discussion of the free volume factor in supercooled liquid dynamics can be found in Reference 74.

When positronium is formed in solids, e.g. glassy polymers or ice, it becomes impossible to push molecules aside to make room for a bubble. Under these conditions positronium can localize in microvoids, called "free volumes". Annihilation with possible captures of positronium in free volumes was first considered by Brandt.<sup>70,75,76</sup> The method offers new possibilities for investigation into the structure of a number of materials, including polymers.<sup>77-82</sup> According to the results<sup>83</sup> the lifetime distributions of positron annihilation in solid molecular systems have more than two components and for amorphous structures they have the following nature:  $\tau_1$  is the component associated with annihilation of singlet Ps, partly with free positron annihilation and annihilation of nonlocalized positronium,  $\tau_2$  is the component of annihilation of free and trapped positrons and non-localized *o*-Ps,  $\tau_3$  is the component of annihilation of localized (captured in microvoids) atoms of triplet positronium. In amorphous-crystalline systems, a spectrum structure becomes more complicated.

#### 4. Pick-off annihilation and polymer structure

According to mentioned above circumstances, this process is determined by the positron spur (Ps formation) and also by the number and size of elementary free volumes (Ps trapping). Consider now a correlation of annihilation characteristics with these parameters.

**4.1. Effective size of elementary free volume and *o*-Ps lifetime.** In some approximation,<sup>62,84-86</sup> a pore can be represented by a spherical potential well with effective radius  $R_3$ . For this case, well calibrated semi-empirical eq 15 represents a dependence of *o*-Ps lifetime  $\tau_3$  on the pore effective radius:

$$\tau_3 = \left\{ \lambda_0^T + 2 \left[ 1 - \frac{R_3}{R_3 + \Delta R} + \frac{1}{2\pi} \sin \left( \frac{2\pi R_3}{R_3 + \Delta R} \right) \right] \right\}^{-1} \text{ (ns)}, \quad (15)$$

Parameter  $\lambda_0^T$  stands here for the intrinsic *o*-Ps annihilation rate ( $0.7 \times 10^9 \text{ s}^{-1}$ ),  $\Delta R = 0.166 \text{ nm}$ , determined by calibration on substances with well known free volume elements and denotes penetration depth of positronium wave function inside of the "walls" of the elementary free volume. The problem of correctness of such estimations, especially in the cases of large (more than 1nm) pores, typical for recently synthesized sorbents and membrane materials still exists. Paper<sup>87</sup> describes such results for the cross-linked polystyrenes and gives a chance to check contemporary models. The names of the sorbents are explained elsewhere.<sup>88</sup> The largest free volume holes in the polymer sorbents (in LPS200X at RT,  $\tau_3 = 73\text{--}75 \text{ ns}$ , and, according to Tao-Eldrup eq 15,  $R_3 = 20 \text{ \AA}$ ) were big enough for comparison with the data of nitrogen sorption experiments. Sorption experiments treated using Brunauer-Emmett-Teller theory.<sup>89</sup> Results for LPS200X are given in Figure 5,<sup>87</sup> and they do not contradict to the positron annihilation lifetime (PAL) estimations given above, though  $R_3 = 20 \text{ \AA}$  is a little bit too large. This comparison along with a discussion of temperature dependence (TD) of annihilation characteristics (Figure 6) were useful for checking possibility to apply contemporary theoretical models, connecting EFV size and positronium lifetimes, to our experimental results. We mean here extended Tao-Eldrup (ETE) model suggested by Goworek et al.<sup>90,91</sup> and so called "classical regime", considering Ps atom as a classical particle in a large hole.<sup>92,93</sup> Analysis of TD-data<sup>87</sup> shows that the classical free path concept for Ps lifetime in a rectangular pore, as well as its modification for spherical or cylindrical pore in CPS150X,<sup>94</sup> LPS200X<sup>87</sup> and also in silica-based glasses (see Figure 2 in Reference 95), though predicting a decrease of the longest leaved *o*-Ps lifetime on heating, does not give good enough fitting to the experimental points over the entire temperature

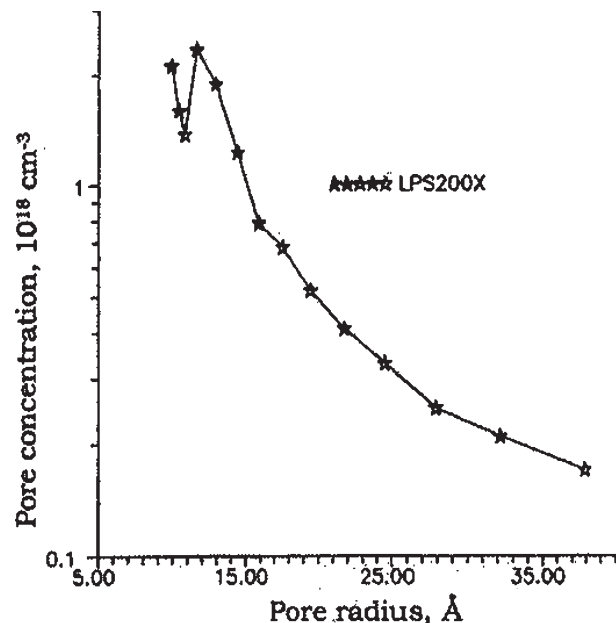


Figure 5. Distribution of the free volume hole sizes in polymeric sorbent LPS200X found from the sorption experiments.<sup>87</sup>

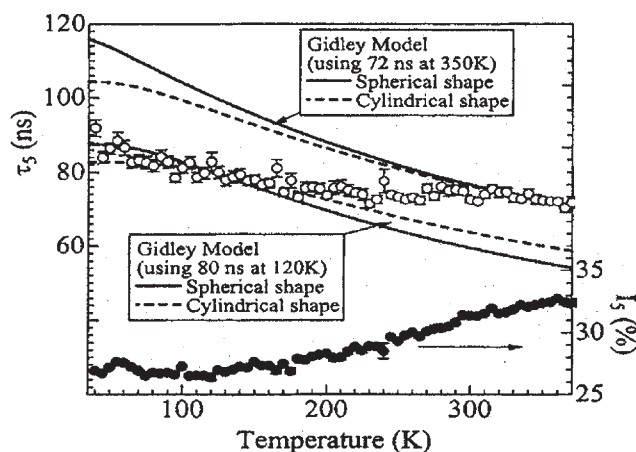


Figure 6. Temperature dependence of the long-lived *o*-Ps component  $\tau_3$ ,  $I_3$  for LPS200X (PATFIT data). Solid lines illustrate different attempts to describe temperature dependence in terms of the classical particle model<sup>87,92,93</sup>

range between 50 and 350 K. *The slope of experimental dependence is too flat compared to the theory.* For example (LPS200X, Figure 6), if the model curve is normalized on high-temperature data, increase of *experimental* lifetime at low temperature is not as strong as it is expected from the theory. For silica-based glasses and polystyrenes, an explanation of this discrepancy was found<sup>88,95,96</sup> in combination of the "large hall" effect with chemical interaction of positronium with radicals induced by irradiation and stored in a sample during the experiment with positron source at low temperature or with atmospheric oxygen strongly trapped between aromatic rings. However, another discrepancy comes out when the estimations of the pore size found on the bases of the ETE model and sorption experiments are compared. The ETE model<sup>91</sup> considers Tao-Eldrup eq 15 as a limiting case of zero temperature. If this idea is followed and we apply this equation to LT data<sup>5</sup> ( $\tau_3 = 100 \text{ ns}$  in LPS200X at 50 K) the pore radius larger than  $25 \text{ \AA}$  is obtained. This size is poorly represented in the distribution in Figure 5 and demonstrate the discrepancy between PAL and sorption data or, more exactly, between the sorption data and results of theoretical estimations made on the bases of the PAL data.

The results obtained show that the effects of Ps annihilation

in the large free volume holes are too complicated and combined PAL and sorption experiments can be very promising for elucidation of this problem.

**4.2. Concentration of elementary free volumes.** This is very important characteristic of various materials determining their mechanical and physico-chemical properties, such as elasticity, aging, permeation, selectivity to different gases, sorption etc. A consideration given here is a simple representation of the idea of *o*-Ps localization in elementary volume of a substance. The simplification is in the assumption that mobility of non-localized positronium before the final trapping is described by some effective diffusion coefficient  $D^{\text{Ps}}$ , and annihilation rate before final localization is taken equal to the free positron annihilation rate:  $\lambda_f^+ = \lambda_f^{\text{Ps}} = \lambda_f$ .<sup>88</sup> In principle, the process can be more complicated: distribution of the spur electrons can be inhomogeneous. Localization can be a process of the consecutive positronium transitions to deeper and deeper traps with longer and longer *o*-Ps lifetimes and, correspondingly, with non-exponential distribution of positronium annihilation. Importance of this effect has to be estimated in each given case from the correctness of multi-exponential fitting. Theoretical considerations of the complicated process can be found in References 97–99.

Generally speaking, a possibility to estimate concentration of elementary free volumes depends on the conditions of formation of localized *o*-Ps. Analytical dependence of the long-lived component intensities on the number of elementary free volumes is important for interpretation of the PAL results. Fraction of positrons, which formed *o*-Ps and is observed as long-lived component in the PAL spectrum, is dependent not only on the number density of EFV (possibility of localization) but also on the density of electrons in positron the spur (possibility of Ps formation). Positrons produce spur electrons during their slowing down. The validity of the spur model of Ps formation in polymers was strongly confirmed recently by experiments on additional Ps formation in irradiated polymers at low temperatures.<sup>45,100</sup> Some results will be discussed later. The model infers that in the case of lack of the spur electrons, no Ps will be formed, though the number of EFV is very high. In addition, precursors of the trapped *o*-Ps can be either non-localized *o*-Ps, or non-localized  $e^+$ , which forms Ps on the spur electron inside or in close vicinity to EFV. This situation can be described by a simple system of kinetic equations (16) where the relation among positronium formation rate  $v_{\text{form}}$ , positronium trapping rate  $v_i^t$ , and annihilation rate of non-localized positronium  $\lambda_f$  determines the choice of the precursor for localized *o*-Ps:

$$\begin{cases} dP_f^+/dt = -(\lambda_f^+ + v_{\text{form}})P_f^+, & P_f^+(0) = 1 \\ dP_f^{\text{Ps}}/dt = (3/4)v_{\text{form}}P_f^+ - (\lambda_f^{\text{Ps}} + \sum_i v_i^t)P_f^{\text{Ps}}, & P_f^{\text{Ps}}(0) = 0 \\ dP_{t,i}^{\text{Ps}}/dt = v_i^t P_f^{\text{Ps}} - \gamma_i P_{t,i}^{\text{Ps}}, & P_{t,i}^{\text{Ps}}(0) = 0 \end{cases} \quad (16)$$

with summing up over the numbers of the long-lived components or over the types of holes ( $i=3, 4$ , etc), and also with  $P_f^+$ ,  $P_f^{\text{Ps}}$ ,  $P_{t,i}^{\text{Ps}}$  standing for the probabilities to find free positron, nonlocalized or trapped positronium, correspondingly;  $\gamma_i = 1/\tau_i$  is the rate of annihilation in the *i*-hole (elementary free volume EFV) and depends on the hole size (see eq 15).

For convenience of discussion, we assign the same label *i* for the lifetime component and for the type of a hole in a sample. In the simplest case of three-component analyses of the PAL spectrum, when only the third component is related with *o*-Ps,  $i=3$ . Transitions between the EFV of different types are neglected. Factor 3/4 in eq 16 is coming because we consider behavior of the long-lived triplet positronium. From eq 16, the intensities of the long-lived components (coefficients before the exponents in the PAL distribution:

$$I_i = (3/4)Q \left\{ v_i^t / (\lambda_f - \gamma_i + \sum_j v_j^t) \right\}, \quad (17)$$

where  $Q = v_{\text{form}} / (\lambda_f - \gamma_i + v_{\text{form}}) \approx v_{\text{form}} / (\lambda_f + v_{\text{form}})$  and is a fraction of positrons forming Ps in a system.

The trapping rate

$$v_i^t = 4\pi D^{\text{Ps}} R_i N_i, \quad (i=3,4, \text{etc.}) \quad (18)$$

where  $D^{\text{Ps}}$  means diffusion coefficient of nonlocalized Ps,  $R_i$  is a radius for interaction, which we suppose equal to the EFV effective radius,  $N_i$  is the number density of trapping centers of a given type.

The condition

$$v_i^t \leq \lambda_f, \quad (19)$$

when some part of nonlocalized *o*-Ps have time to annihilate before trapping, implies nonlocalized *o*-Ps as a precursor of localized *o*-Ps, when intensities of the long-lived positronium components  $I_i$  are dependent on the concentration  $N_i$  and radius  $R_i$  of the holes of corresponding type (see eq 17). This is *the first case* in terms of the previous qualitative discussion. For the PAL spectrum with one long-lived component ( $\tau_3, I_3$ ),  $v^t$  can be expressed also in terms of annihilation characteristics as

$$v^t = 4\pi D^{\text{Ps}} R_3 N_3 = (4I_3/3)(\lambda_f - \gamma_3) / (Q - 4I_3/3) \approx (4I_3/3)(\lambda_f - \gamma_3) / (I_1 - I_3/3) \quad (20)$$

The accurate values of  $D^{\text{Ps}}$  in a given polymer are not known. However, Jean et al.<sup>101</sup> had found  $D^{\text{Ps}} = 0.2 \times 10^{-4} \text{ cm}^2/\text{s}$  for positronium in the bulk of the porous resins. An attempt was made to estimate diffusion coefficient of non-trapped Ps in a polymer bulk using positron annihilation data for the porous poly(phenylene oxide) with the known specific surface area, and it was found that  $0.5 \times 10^{-4} < D^{\text{Ps}} < 1.5 \times 10^{-4} \text{ cm}^2/\text{s}$ .<sup>102-104</sup> We suppose that scattering of the data may cover the difference in the mobility of non-localized Ps atom in the most of polymer materials, though this uncertainty decreases precision of the results. In principle, the data from this range and annihilation characteristics  $\tau_3, I_3$  can be used in eq 20 for estimation of  $N_3$  in various polymers, if the relation (19) is fulfilled. Obviously, the diffusion coefficient for *nonlocalized* positronium  $D^{\text{Ps}}$  is different from that for *localized* positronium. The last parameter was estimated as  $(2.6-3.2) \times 10^{-6} \text{ cm}^2/\text{s}$  by Hirata et al.,<sup>105</sup> from the results on positronium quenching by dinitrophenyl in amorphous polysulfone, polycarbonate and polystyrene.

The *second case* (see discussion above) implies that

$$v_i^t \gg \lambda_f. \quad (21)$$

In fact, validity of this condition means that free positron is a precursor of localized *o*-Ps.

From eq 17

$$I_i = (3Q/4) v_i^t / \sum_j v_j^t = (3Q/4) R_i N_i / \sum_j R_j N_j. \quad (22)$$

For two types of the holes  $k$  and  $m$ , for example,

$$I_k / I_m = R_k N_k / R_m N_m. \quad (23)$$

When the specific surface area  $S$  of the sample is known, and it is determined mostly by the largest EFV ( $S \approx S_m \approx 4\pi R_m^2 N_m$ ), eq 5 can be used for calculations of  $N_k$ .<sup>88</sup>

However, if there is only one long-lived component (one type of elementary volumes), intensity of the long-lived component depends only on  $Q$  ( $I_3 = 3Q/4$ ), and it can not be related directly to concentration of EFV. Sometimes it is not obvious what condition, eq 19 or 21, is valid and, furthermore, it is known

that  $I_3$ , the only long-lived component in a system, can be influenced by the positron trapping with an acceptor, like polar carbonyl group. To avoid this uncertainty and to calculate the number density of free volume holes in this case, temperature dependence of  $o$ -Ps lifetime  $\tau_3$  below and above the glass-transition temperature  $T_g$  might be used.<sup>106,107</sup>

Let us consider the effect of temperature on the free volume characteristics of polymers. The coefficient of thermal expansion of the total volume  $\alpha$  can be written as

$$\alpha = \alpha_h h + \alpha_b (1-h), \quad (24)$$

where  $h$  is fractional free or hole volume ( $V_h/V$ ),  $\alpha_i$  are thermal expansion coefficients of the holes (subscript “ $h$ ”) and of the bulk (subscript “ $b$ ”). Hence,

$$h = (\alpha - \alpha_b) / (\alpha_h - \alpha_b) \quad (25)$$

Hristov et al.<sup>108</sup> had shown that eq 25 can be applied both in the temperature ranges  $T < T_g$  and  $T > T_g$ . Assuming also that  $h$  behaves continuously at  $T_g$  and  $\alpha_b (T < T_g) = \alpha_b (T > T_g)$ , the value  $\alpha_b$  can be eliminated, and for  $T \rightarrow T_g$

$$h_g = (\alpha_r - \alpha_g) / (\alpha_{h,r} - \alpha_{h,g}). \quad (26)$$

Parameters  $\alpha_r$  and  $\alpha_g$  (with subscripts “ $r$ ” for rubber and “ $g$ ” for the glass phases) are related to macroscopic volume while  $\alpha_{h,r}$  and  $\alpha_{h,g}$  describe behavior of the hole volumes.

Now, in the case when  $\alpha_r$  and  $\alpha_g$  for a given polymer are not known, the Simha-Boyer value  $(\alpha_r - \alpha_g) T_g \cong 0.113$  may be used,<sup>109</sup>

$$h_g = 0.113 / \{T_g (\alpha_{h,r} - \alpha_{h,g})\}, \quad (27)$$

and the fractional free volume  $h_g$  at  $T = T_g$  can be found from eq 27 using only positron annihilation data. From  $h_g = v_g N_g$  we estimate the number density of holes  $N_g = h_g / v_g$  at this temperature. It seems to have been demonstrated now<sup>106</sup> that in the amorphous phase the hole volume fraction  $h(T)$  is controlled mainly by the temperature dependence of the mean hole volume  $v_a$ , and the proportional constant, that is the number  $N$  of holes per  $\text{cm}^3$ , does not depend much on temperature, i.e.  $h(T) = N v_a(T)$  so that  $N \cong N_r \cong N_g$ . Further testing of this assumption may be in so called pressure-volume-temperature (PVT) experiments.<sup>110</sup>

**4.3. Typical examples.** Calculations using eq 27 can be illustrated on example of some polyimides, particularly PI189 and PI304.<sup>111</sup> This example is interesting since in many polymers, as it will be seen below, initial structure is not stable and irreversibly changing under influence of the temperature. This is shown in Figure 7 for PI189. Only on the second cycle of heating above glass transition temperature  $T_g = 165^\circ\text{C}$  temperature dependence of annihilation characteristics becomes, what we shall call, “regular” (Figure 8) and corresponding to linear variations of the elementary volumes of the free volume elements below ( $v_{h,g}$ ) and above ( $v_{h,r}$ )  $T_g$  (Figure 9). These volumes were found from the hole radius  $R_3$  ( $o$ -Ps lifetimes  $\tau_3$ ). The dependence shown in Figure 9 makes it possible to determine thermal expansion coefficients of holes occupied by Ps in the rubbery ( $r$ ) and glassy ( $g$ ) phases.

$$\begin{aligned} \alpha_{h,r} &= (1/v_{h,r}) dv_{h,r} / dT = 95.5 \times 10^{-4} \text{K}^{-1}, \\ \alpha_{h,g} &= (1/v_{h,g}) dv_{h,g} / dT = 3.9 \times 10^{-4} \text{K}^{-1}. \end{aligned} \quad (28)$$

Naturally,  $\alpha_{h,g} \ll \alpha_{h,r}$ . According to positron annihilation data,  $T_g$  for PI189 is readily found from the crossing point of the slopes for the glass and rubber phases. It comes equal to  $160^\circ\text{C}$ , which is in agreement with literature. Combination of eqs 27 and 28 gives  $h_g = 3.35\%$ , and at the glass transition tempera-

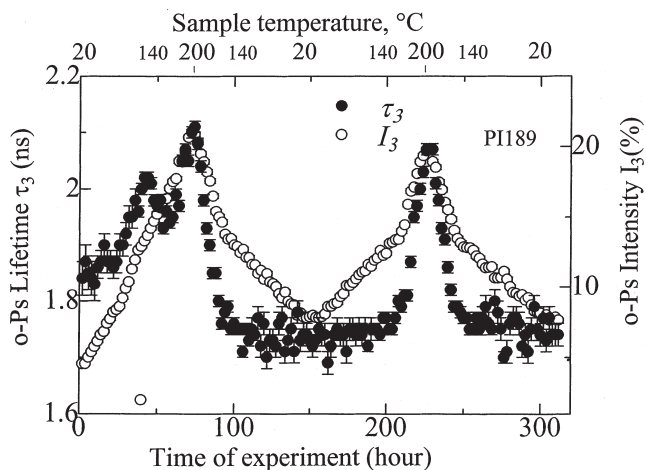


**Figure 7.** Variation of annihilation characteristics  $I_3$ ,  $\tau_3$  in PI189 as function of the time of measurements (temperature) for two cycles of measurements ( $20^\circ\text{C} \rightarrow 200^\circ\text{C} \rightarrow 20^\circ\text{C}$ ). Each point corresponds to two hours of measurements and to variation of sample temperature by  $5^\circ\text{C}$ . Non-regularity is seen between  $125$  and  $165^\circ\text{C}$ .

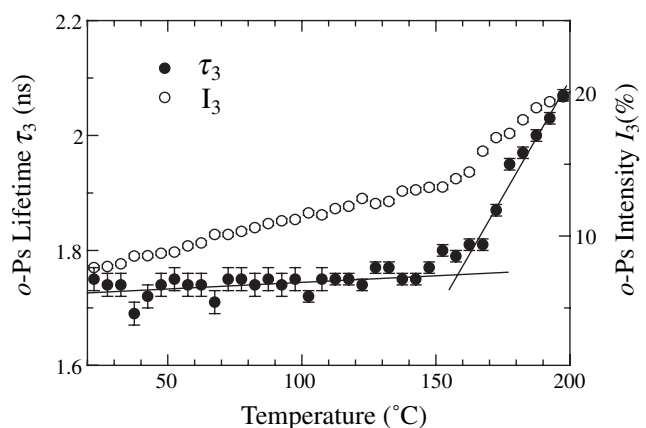


**Figure 8.** Dependence of  $I_3$ ,  $\tau_3$  on temperature for PI189. Heating stage of the second cycle ( $20^\circ\text{C} \rightarrow 200^\circ\text{C}$ ).

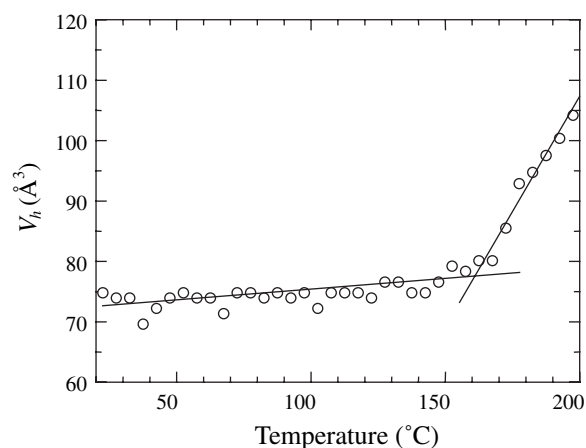


**Figure 9.** Effect of temperature on the hole volume  $v_h$  in PI189 calculated using the data from Figure 7 and equation eq 17.<sup>87</sup>

ture  $N_g = h_g / v_g = 0.44 \times 10^{27} \text{m}^{-3}$ . For comparison, according to Reference 106, similar approach gives for PE and PTFE  $0.73 \times 10^{27} \text{m}^{-3}$  and  $0.36 \times 10^{27} \text{m}^{-3}$ , respectively.

The case represented by eq 23 can be illustrated on example of polymers with highly developed free volume and specific surface, cross-linked polystyrenes<sup>96</sup> (Table 4, see also sec. 4.1). Effective radius of the voids is readily found from eq 15, and for LPS-150X, for example,  $R_3 = 2-3 \text{Å}$ ,  $R_4 = 5 \text{Å}$ ,  $R_5 = 15 \text{Å}$ . Since  $R_5$  is essentially larger than  $R_3$  and  $R_4$ , density  $\rho$ , specific sur-

**TABLE 4: Annihilation characteristics  $\tau_i$ ,  $I_i$  at room temperature, specific surface  $S_L$  and  $S_{BET}$ , density  $\rho$  and the largest radius of nanopores  $R_5$  sensed by positronium in some of the cross-linked polystyrenes**

substance	$\tau_3$ , ns $I_3$ , %	$\tau_4$ , ns $I_4$ , %	$\tau_5$ , ns $I_5$ , %	$R_5$ , Å	$\rho$ , g/cm <sup>3</sup>	$S_L$ , m <sup>2</sup> /g	$S_{BET}$ , m <sup>2</sup> /g
CPS(0.3)-100E, vac	1.23±0.05 6.76±0.24	5.58±0.11 7.67±0.10	39.49±0.28 15.00±0.06	13	0.76	1000	718
CPS(0.3)-150E, vac	1.69±0.15 7.27±0.37	5.31±0.32 8.33±0.33	16.56±0.33 9.52±0.33	8	0.71	1200	972
CPS(0.3)-150E, nitr	1.84±0.15 5.69±0.27	6.81±0.34 8.25±0.22	21.58±0.42 10.33±0.32	10			
LPS150X, vac	1.23±0.06 5.47±0.22	6.12±0.17 5.20±0.09	52.13±0.24 29.29±0.06	15	0.60	1600	965

face  $S$ , and fractional free volume of the porous samples  $V_f$  is determined mostly by the largest voids ( $R_5$ ).

$$V_f = (\rho_{Ps} - \rho_{150}) / \rho_{Ps} = 0.429 ; N_5 = 3V_f / 4\pi R_5^3 = 3 \times 10^{19} \text{ cm}^{-3} \quad (29)$$

Correspondingly, from eq 23 for LPS150X  $N_4 = 1.45 \times 10^{19} \text{ cm}^{-3}$  and  $N_5 = 3.36 \times 10^{19} \text{ cm}^{-3}$ . Along with results of five-term analyses of the PAL spectra, largest hole radius  $R_5$  and density  $\rho$ , Table 4 contains also specific surface area determined from thermal desorption of argon and using Langmuir formula ( $S_L$ ) and also from nitrogen sorption measurements ( $S_{BET}$ ) combined with BET theory.<sup>89</sup> Estimation of  $N_5$  from the equation  $N_5 = S_L / 4\pi R_5^2$  gives about the same value as in eq 29. On the other hand, BET theory and Kelvin equation,<sup>89</sup> applied to data on nitrogen sorption makes it possible to obtain size distribution of EFV in samples from Table 4 shown in Figures 10 and 11 at  $R > 10$  Å. Remarkably, PAL estimation  $R_5 = 15$  Å is just in a middle of this distribution. Integration of the distribution for LPS150X in the vicinity of  $R_5 = 15$  Å gives concentration of voids  $2.5 \times 10^{19} \text{ cm}^{-3}$  which corresponds to the estimation given above. Thus, combined application of PAL and BET techniques mutually confirms obtained results and extends the ranges of the pore diagnostics in polymers.

**4.4. Effect of low-temperature Ps formation.** Low-temperature positronium formation in polymer is known since nineties.<sup>45,112-117</sup> Not referring to all publication, we wanted to mention some ideas important for understanding of this effect, since it came out to be useful in the polymer structure investigations. The authors<sup>114</sup> suggested a qualitative explanation of additional Ps formation by interaction of positrons with weakly bound electrons, produced by preliminary  $\gamma$ -irradiation or by irradiation during the positron annihilation experiment and localized at low temperature. Simple quantitative consideration of this effect for PE and PMMA polymers was given in Reference 116 on the bases of the same system of kinetic equations, eq 16. The only difference is in the zero moment condition in the equation for positrons:  $P_f^+(0) = 1 - Q$ , where  $Q$  is a fraction of the positronium formed in a polymer without  $\gamma$ -irradiation. The rest of the positrons ( $1 - Q$ ) escape from the spur and have a chance to form Ps on the trapped electrons. The solution of the corrected system of eq 16 gives an increase in  $I_3$ ,  $\Delta I_3$  due to additional Ps formation on the trapped electrons:

$$\Delta I_3 = (3/4)(1 - Q)v_{\text{form}}(\lambda_f + v_{\text{form}} - \gamma_3)^{-1}v_T(\lambda_f + v_T - \gamma_3)^{-1} = (3/4)(1 - Q)AB, \quad (30)$$

where  $B = v_T(\lambda_f + v_T - \gamma_3)^{-1}$  and meaning of  $A$  is obvious from eq 30;  $v_{\text{form}} = 4\pi D_f^+ R N_e = k_{\text{form}} N_e$  and  $v_T = 4\pi D_f^{\text{Ps}} R_3 N_3$ . Parameters  $D_f^+$  and  $D_f^{\text{Ps}}$  are diffusion coefficients of free  $e^+$  and Ps, correspondingly;  $R$  is effective radius for interaction of  $e^+$  and trapped electron, and  $R_3$  describes effective size of the trapping center.

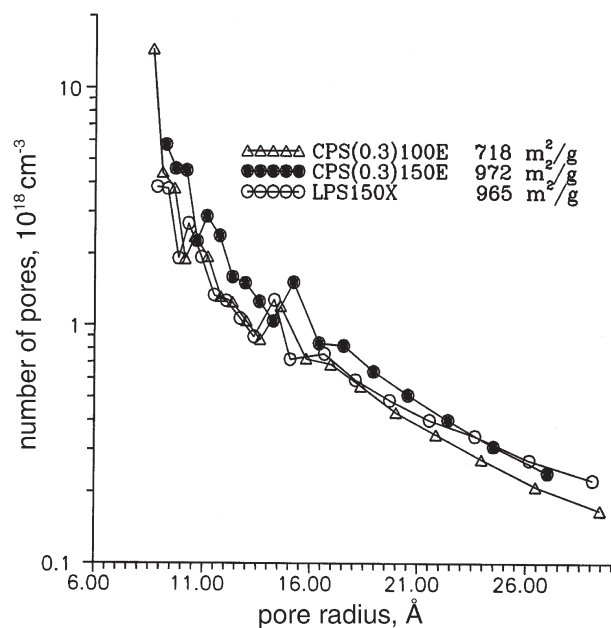


**Figure 10.** Size-distribution of pores in cross-linked polystyrenes from Table 4 obtained from incremental pore area data (BET).<sup>96</sup>

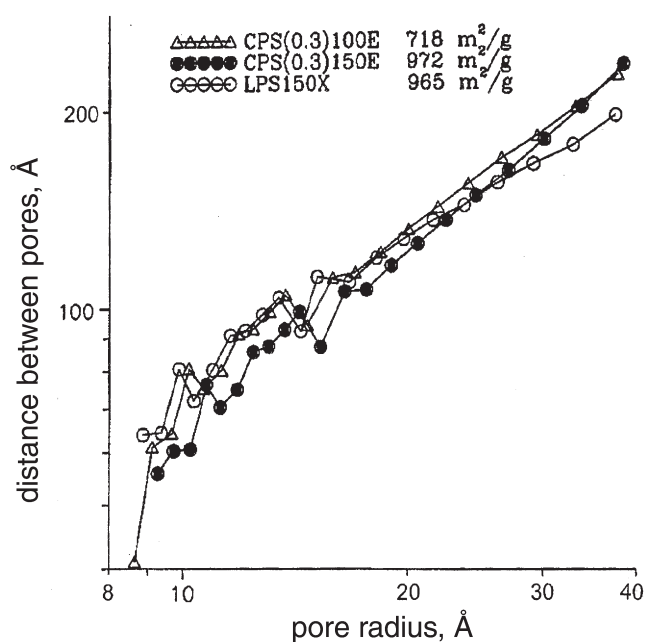


**Figure 11.** Distance between pores, calculated from the data shown in Figure 9.<sup>96</sup>

It becomes obvious that fitting of eq 30 to experimental points for PE<sup>114</sup> is possible only with  $k_{\text{form}}(\text{PE}) = v_{\text{form}}/N_e = 10^{-7} \text{ cm}^3/\text{s}$  and  $v_T \gg \lambda_f$ , i.e.  $B=1$  (Figure 12). A description of the PMMA results for the highest  $N_e = 2 \times 10^{17} \text{ cm}^{-3}$ <sup>114</sup> is possible by suggesting the two following alternatives:

(a)  $v_T \gg \lambda_f$ ,  $B=1$ ,  $k_{\text{form}}(\text{PMMA}) = (1/50)k_{\text{form}}(\text{PE}) = 0.24 \times 10^{-8} \text{ cm}^3/\text{s}$ . The last ratio probably means that  $D_f^+(\text{PMMA}) = (1/50)D_f^+(\text{PE})$ . The diffusion coefficient for PE at 30 K is known to be about  $0.1 \text{ cm}^2/\text{s}$ .<sup>118</sup> Therefore, the positron diffusion coefficient at 30 K in PMMA is about  $0.002 \text{ cm}^2/\text{s}$ . This result corresponds to recently published data.<sup>119</sup>

(b)  $v_T$  and  $\lambda_f$  are comparable. Fitting to the highest value of  $\Delta I_3$  gives the probability of Ps trapping  $B = 0.2$ , if the rate constant of Ps formation on the trapped electrons in PE and PMMA are roughly the same:  $k_{\text{form}}(\text{PMMA}) = k_{\text{form}}(\text{PE}) = 10^{-7} \text{ cm}^3/\text{s}$ .

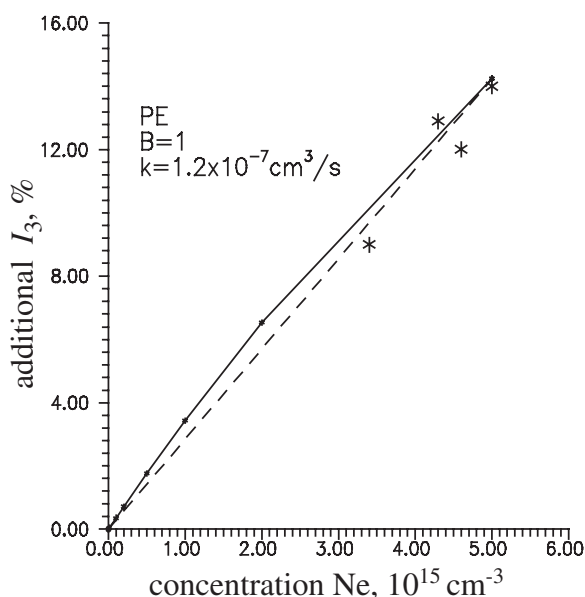


**Figure 12.** Additional intensity  $\Delta I_3$  of the longest lifetime component in PE as a function of the trapped electron density.<sup>114</sup> The dependence is described (solid line) by eq 30 with  $k_{\text{form}}(\text{PE}) = 1.2 \times 10^{-7} \text{ cm}^3/\text{s}$  and  $B = 1$ . The dashed line here and in Figure 13 shows linear dependence for comparison.

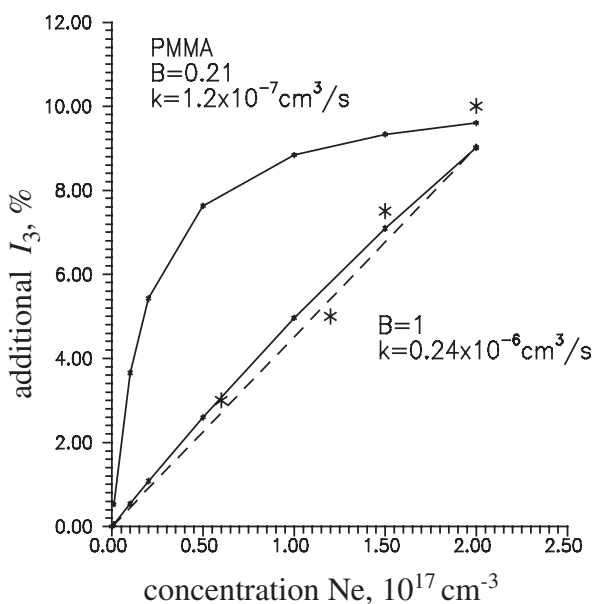


**Figure 13.** Additional long-lived component intensity  $\Delta I_3$  as a function of the trapped electron density<sup>114</sup> in PMMA. Solid curves correspond to different sets of parameters in eq 30.  $k_{\text{form}}(\text{PMMA}) = k_{\text{form}}(\text{PE}) = 1.2 \times 10^{-7} \text{ cm}^3/\text{s}$ ,  $B = 0.21$  or  $k_{\text{form}}(\text{PMMA}) = (1/50)k_{\text{form}}(\text{PE}) = 0.24 \times 10^{-8} \text{ cm}^3/\text{s}$  and  $B = 1$ .

A comparison of calculated dependences for the two cases mentioned above is given in Figure 13.

We have to conclude that for PMMA, just as for PE, the alternative (a) gives a much better description of the whole set of points<sup>114</sup> than the alternative (b). And this is the first direct argument in favor of the point of view that in such polymers as PE and PMMA all *o*-Ps atoms are probably trapped before annihilation ( $B = 1$ ). It means that in such cases  $I_3$  is dependent mostly on the probability of Ps formation in a substance  $Q$  but not on the number of the trapping sites  $N_3$ , since the number of Ps traps is too high ( $v_T \gg \lambda_f$ ). Further experiments of this type could be useful. In the scope of the further study of the mechanism of Ps formation on the trapped electrons, a comparison of the observed effect with results on thermo-stimulated luminescence (TSL) for the same samples at low temperatures was suggested in Reference 116. In agreement with the described results, integral TSL intensity (Figure 14) for PE is much higher than for PMMA, since both effects, additional Ps formation and TSL are determined by the amount and stability of the weakly bound electrons.

**4.5. Some cases when free Ps trapping rate and annihilation rate are comparable.** It follows from the previous section that in PE and in PMMA most of *o*-Ps atoms are trapped before annihilation (relation 21 from sec. 4.2 is fulfilled). How typical is this situation for solid substances, and are there any cases when some of *o*-Ps atoms have chance to annihilate before final localization (relation 19 in sec. 4.2)? The problem with polymers will be discussed below. However some examples can be found now among solid organic substances. In solid biphenyl for example, *o*-Ps intensity  $I_3$  decreases to zero at pressure about  $10^8 \text{ Pa}$ .<sup>120,121</sup> Probably, due to compression, elementary free volume size is reduced below the value, when the quantum level for positronium in the well can exist. In other words, *o*-Ps is not localized before annihilation.

Another example is found among highly dispersed polycrystalline oxides and salts of metals.<sup>122</sup> Hydroxyapatite  $\text{Ca}_{10}(\text{PO}_4)_6(\text{OH})_2$ , vaterite  $\text{CaCO}_3$  and also  $\text{CaSO}_4$  and  $\text{Al}_2\text{O}_3$  are the materials where the intensity of extremely long (20–60 ns) lifetime component of relatively low intensity depends not only on the probability of *o*-Ps formation inside of the microcrystallite, but also on the probability of this atom to diffuse to microcrystallite surface and to localize inside of the intercrystallite space. It was seen from the fact that increase of the effective size of crystallites after annealing was found to inhibit long-lived *o*-Ps component because this enlargement prevents positronium localization. Experiments<sup>122</sup> are interesting also by comparison of positron annihilation and sorption data. As

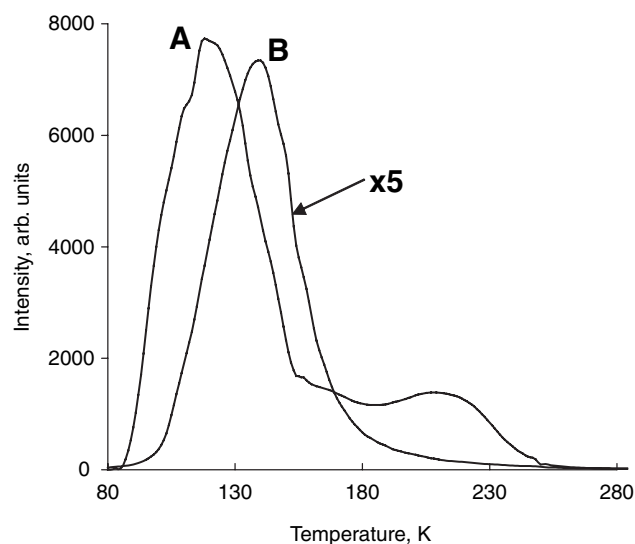


**Figure 14.** Integral intensity of the TSL curves for PE (A) and PMMA (B). Both curves are represented in the same relative scale.<sup>116</sup>

it was discussed above for cross-linked polystyrenes, data on low-temperature nitrogen sorption enable calculation of size-distribution of elementary free volumes in a system. This distribution for vaterite is shown in Figure 15. Lifetime measurements indicate that positronium is sensitive only to the left part of this distribution: experimental lifetime of localized positronium  $\tau_4 = 22.87 \pm 2.36$  ns corresponds to pore radius  $R \approx 10$  Å and number density of free volume holes (intercrystallite spaces)  $N_4 = (2-3) \times 10^{16} \text{ cm}^{-3}$ . This concentration gives average distance between inter-crystallite spaces  $\sqrt[3]{1/N}$  attainable for positronium atom (see also Figure 11) and, correspondingly, positronium diffusion length  $L$ . In the result, diffusion coefficient  $D_{\text{cryst}}^{\text{Ps}} = L^2/\tau$  of non-localized Ps in a crystallite can be found  $0.4 \times 10^{-1} \text{ cm}^2/\text{s}$ . Amorphization leads to strong decrease of positronium mobility. Comparison of the results of sorption experiments in polymer glasses (Figures 5 and 10) and crystallites (Figure 15) show that in disordered structures positronium is three orders of magnitude less sensitive. It is trapped by pores having three orders of magnitude higher concentration (about  $3 \times 10^{19} \text{ cm}^{-3}$ ). This means three orders of magnitude lower mobility ( $D_{\text{grass}}^{\text{Ps}} = 0.4 \times 10^{-4} \text{ cm}^2/\text{s}$ ). These values and eq 20 give, for example, in polycrystalline  $\alpha\text{-Al}_2\text{O}_3$   $N_4 = 1.14 \times 10^{16} \text{ cm}^{-3}$  for the number density of inter-crystallite spaces and  $N_3 = 9.7 \times 10^{19} \text{ cm}^{-3}$  in amorphous  $\text{Al}_2\text{O}_3$  for the number density of defects.

## 5. Polymer structure as seen by positron annihilation

**5.1. Structural transitions.** A study of temperature dependence of annihilation characteristics (and low-temperature Ps formation) became a useful instrument for investigations of structural transitions in polymers. The intermolecular spaces available for localizing positronium are situated mostly in the amorphous regions and crystalline-amorphous interfaces. Generally, a transition of a polymer from one state to another is accompanied by changes in thermal expansion coefficient of the material, which influences directly the thermal expansion coefficient of the free volume holes. Consequently, by investigating the lifetime changes as a function of temperature, the transitions could be observed. As soon as polymer segmental motion, which is frozen at low temperature, commences by heating polymer samples above the relaxation temperature, the shallow potentials are smeared out. Then the trapped electrons in shallow potentials are excited, resulting in the reduction of the amount of electrons available for Ps formation. Hence, this contributes to the decrease in the Ps formation. In such a way,

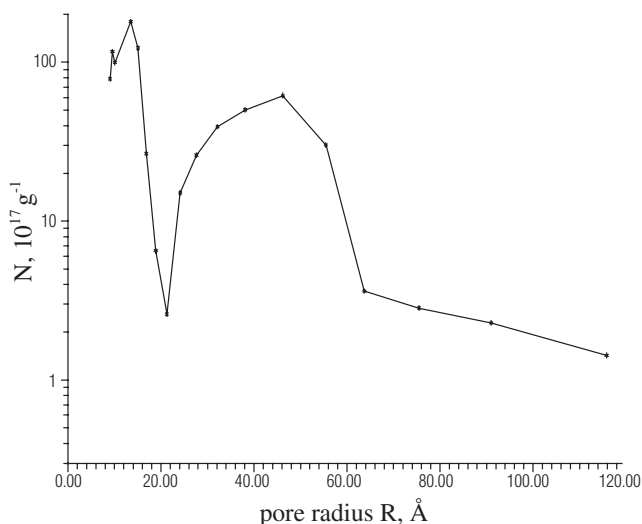


**Figure 15.** Size-distribution of elementary free volumes (inter-crystallite sites) in vaterite ( $\text{CaCO}_3$ ) polycrystal obtained from low-temperature sorption isotherm of nitrogen gas (Brunauer-Emmett-Teller BET method).<sup>122</sup>

by monitoring the *o*-Ps intensity, an onset of a new motion of some parts of the polymer-chain below the glass-transition temperature could be detected in polypropylene (see Figure 16<sup>95</sup>). When the temperature of measurements is higher than  $T_g$ , the polymer is in rubbery state, and large molecules in the amorphous regions can move like in viscous liquid, and Ps probe manifests its nature simultaneously to be a seeker and a digger of free volume holes, and could expand additionally the free-volume hole where it is localized. As the temperature increases, and, due to thermal expansion, more and more free-volume holes become available for localization of Ps, sharp increase of the *o*-Ps intensity  $I_3$  is observed (Figure 16). In this way, structural transformations in PP were observed. The identification of transition and relaxation temperatures can be done according Krevelen and Hoftyzer<sup>123</sup>:  $T_\gamma$ :  $\gamma$  relaxation, rotation of the methyl group,  $T_\beta$ :  $\beta$  relaxation, motion of very small section of polymer chain,  $T_g$ : glass transition (lower), main chain local motion which arise from purely amorphous material,  $T_{gu}$ : second (upper) glass transition, main chain local motion which arises from amorphous material which is under restraint due to the vicinity of crystallites,  $T_{ac}$ : premelting transition, hindered rotation of polymer chains inside the folded crystals, and  $T_m$ : melting point. It is very difficult to estimate precisely the error of determination of the corresponding values, but it is probably not higher than 5 K.

**5.2. Heterogeneity of polymeric systems.** Elastic and glassy polymers are normally considered as homogeneous disordered materials with unimodal (statistical) distribution of elementary free volumes. In this paragraph, we discuss results of PAL measurements for a number of elastic and glassy polymers, where observations of the two long-lived *o*-Ps components in the PAL spectra and irregular (nonlinear, see sec. 4.3) variations of annihilation characteristics in the vicinity of glass transition temperature reveal structural heterogeneity of these systems. The conclusion is confirmed by measurements of TSL, thermo-mechanics and mobility of penetrants.

Elementary free volumes, the carriers of the free volume in materials, are very important characteristic of the matter, determining such properties as permeability, swelling ability, selectivity, mechanical strength, etc. It is generally accepted to consider polymers in glassy and elastic states as homogeneous disordered materials with unimodal, statistical distribution of elementary free volumes. Positron annihilation lifetime measurements give a chance to check this point of view. If size distribution of elementary free volumes is one-centered (only one average effective radius), PAL distribution, analyzed with the known mathematical programs PATFIT or MELT, will include only one long-lived (several nanoseconds) *o*-Ps component. Observation of two or more long-lived components in a

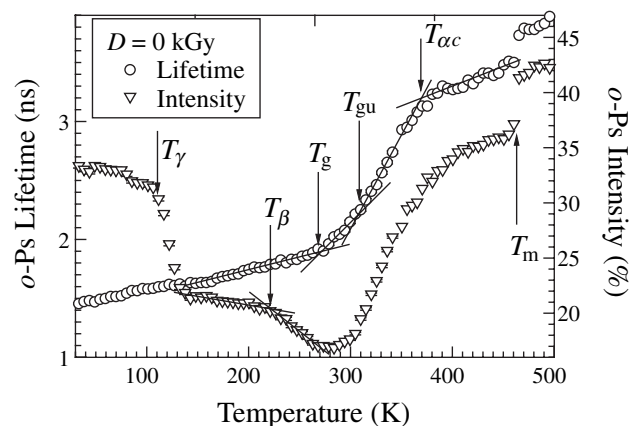


**Figure 16.** *o*-Ps lifetime and intensity versus temperature for polypropylene.<sup>95</sup>  $T_\gamma$ :  $\gamma$ -relaxation temperature,  $T_\beta$ :  $\beta$ -relaxation,  $T_g$ : glass transition (lower),  $T_{gu}$ : glass transition (upper),  $T_{ac}$ : pre-melting transition,  $T_m$ : melting point.

rubber or polymer glass would mean inhomogeneity of corresponding material. However the number of the long-lived Ps components is not obvious sometimes. Thus, it was demonstrated recently<sup>124,125</sup> that, in the cases of small (about 2 ns) difference between two lifetimes or between two peaks in the probability density function of positron annihilation with a given lifetime (obtained from the MELT program), the splitting can be an “artefact”, i.e. a result of incorrect mathematical treatment (deconvolution) of experimental non-exponential lifetime distribution of positron annihilation. Nevertheless, we are interested in revealing heterogeneity of amorphous polymers in principle. Therefore, we concentrate here on the PALS data for a number of polymers, such as polyisobutylene, polybutadiene, synthetic rubbers, cross-linked polystyrene, where observation of the two long-lived positronium components in the spectrum (bi-central distribution) corresponds to the signs of heterogeneity of these compounds, obtained by supplementary techniques, such as TSL, X-ray scattering, mobility of the marker, thermo-mechanics and demonstrates heterogeneity of these materials. Being considered together, the experimental results corroborate the idea of heterogeneity of some of the studied structures.

**Cross-linked polystyrene.** Typical probability density function of different positronium lifetimes in the cross-linked networks CPS200E and LPS200X (References 96 and 126, see also sec. 4.1) is given in Figure 17. Three groups of lifetimes (three effective sizes of EFV) are clearly resolved:  $\tau_3=1.5$  ns with the intensity  $I_3=2.3\%$ ;  $\tau_4=7.4$  ns and  $I_4=2.8\%$ ;  $\tau_5=73$  ns and  $I_5=32\%$ . According to eq 15, these lifetimes correspond to the following effective radius of the free volumes:  $R_3=2-3$  Å,  $R_4=6$  Å and  $R_5=20$  Å. On the other hand, mechanical tests

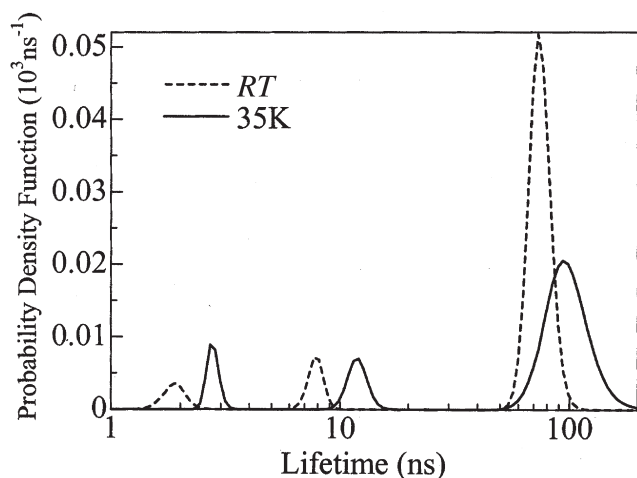


**Figure 17.** Probability density function of positron annihilation with a given lifetime (MELT results) for hyper-cross-linked polystyrene network<sup>96,125</sup> at different temperatures (RT and 35 K).

(under compression) were performed for such super-cross-linked polystyrenes (CPS(0.3)100E and CPS(0.3)200E) fully swollen in water and kept at different temperatures.<sup>127</sup> The derivative ( $dh/dT$ ) of the spherical bead diameter  $h$  at different temperatures and given pressure is shown in Figure 18. Curves 1 and 2 are related to mentioned swollen polystyrenes and curve 3 for the dry CPS(0.3)100E is reproduced for comparison. Curve 4 related to the pure ice, obtained by crystallization of water onto a quartz plate at  $-150-100$  °C. At least two peaks  $dh/dT$  are clearly seen for each sample at the same temperatures. It seems reasonable that these peaks correspond to different plastification effects of water in free volumes, characterized by inhomogeneous size-distribution and measured for the first time by positron annihilation technique.

**Rubbers.** We suggest to consider reliable measurement of the two long-lived *o*-Ps components as an argument in favor of heterogeneity of amorphous polymers. This point is illustrated on example of polymer rubbers. Table 5 contains the longest-lived positronium components obtained from the PATFIT unconstrained four-component analyses of PAL spectra for the rubbers. Left part of the Table 5 includes materials described well in terms of the two long-lived *o*-Ps components. This description gives better fitting and characteristics of the components have a good precision. In the right part of the Table 5, there are materials for which description in terms of the two long lifetimes is not necessary: uncertainty of the longest lifetime intensity is too high. Therefore, in the frames of the previous discussion, positron annihilation method considers the following group of substances as heterogeneous systems: *cis*-1,4-polybutadiene (*cis*-1,4-PB); polyisobutylene (PIB), i.e. a copolymer of isobutylene and isoprene; polybutadiene (SKB);

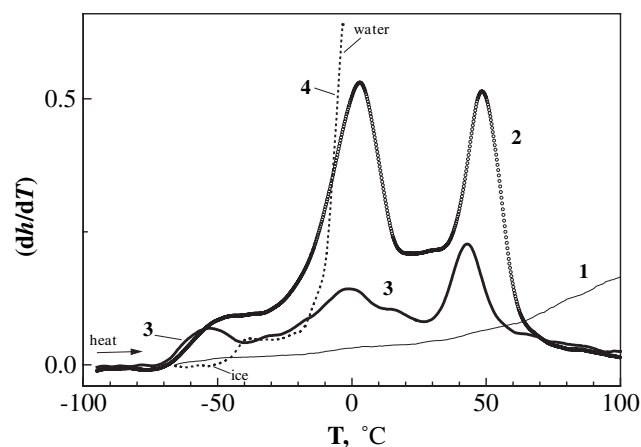


**Figure 18.** Derivative thermo-mechanical curves  $dh/dT$  for spherical beads of the hyper-cross-linked polystyrene CPS(0.3)100E (1) and also for this polymer (2) and CPS(0.3)200E (3) fully swollen in water, and (4) ice on a quartz plate, crystallization at  $-150-100$  °C.<sup>127</sup>

**TABLE 5: Longest-lived *o*-Ps components obtained from the PATFIT unconstrained four-component analyses for a number of rubbers**

Inhomogeneous structure			Homogeneous structure		
Substance	$\tau_3$ , ns $I_3$ , %	$\tau_4$ , ns $I_4$ , %	Substance	$\tau_3$ , ns $I_3$ , %	$\tau_4$ , ns $I_4$ , %
PIB	1.59±0.11	2.68±0.12	BNKS-40	1.66±0.60	2.51±0.29
$\phi=50\%$	18.66±2.67	13.67±2.97	$\phi=31\%$	8.33±6.68	11.0±8.09
PIB, 180C annealed	1.51±0.22 11.90±2.47	2.55±0.15 11.42±3.41	BNKS-40 Ann. 90C	1.95±0.10 14.17±0.52	3.95±1.0 0.93±0.87
<i>cis</i> 1,4 PB	1.29±0.59	2.66±0.05	PI	2.28±1.06	3.01±0.39
$\phi=13\%$	4.54±1.50	24.50±1.85	$\phi=25\%$	10.09±25.02	23.28±25.62
SKB	1.59±0.48	2.95±0.11	BNKS-28	2.02±0.16	3.54±0.70
$\phi=69\%$	6.80±1.88	17.43±2.99	$\phi=47\%$	13.8±1.6	2.24±2.05
BNKS-18	1.65±0.39	2.82±0.17			
$\phi=37\%$	7.00±2.27	10.25±3.09			

a copolymer of acrylonitrile ( $x$ ) and butadiene ( $1-x$ ) (BNKS) with  $x=18\%$ . This conclusion is confirmed using TSL technique. According to this method, materials from the left side of the Table 5 have two glass-transition temperatures: 174/177 K for *cis*-1,4-PB; 230/233 K for PIB; 210/225 K for SKB, and 226/246 K for BNKS (18%). Figure 19 gives a typical example of  $T_g$  splitting in BNKS (18%) compared to BNKS(28%) and BNKS(40%). In addition, heterogeneity of *cis*-1,4-PB was revealed with so called mobility (penetration) technique by measuring variations of permeation activation energy  $E_D$  of penetrant with temperature. Thus, for the penetrant diphenylguanidine (DPhG), this variation (from 32.3 to 57.4 kJ/M) was found above  $T_g$  at 65 °C. This increase of  $E_D$  with heating is not expected in the frames of simple free volume model for homogeneous structure and can be related with the increase of the volume content  $\phi$  (Table 5) of the ordered sites of smaller permeation, i.e. in fact, by phase transformation of the inhomogeneous rubber structure.

**Polystyrene.** Examples of temperature dependence of positronium annihilation characteristics in polystyrene (PS) samples with different molecular weights  $MW=3.6 \times 10^3$  and  $8 \times 10^5$  are shown in Figures 20 and 21. Irregular variation of intensity  $I_3$  of the long-lived Ps component in PS ( $MW=3.6 \times 10^3$ , Figure 20) on heating above  $T_g$  (well defined by the typical bending of  $\tau_3$  at 75 °C) correspond to structural transformations of the rubber in this temperature range. For PS with  $MW=8 \times 10^5$  (Figure 21), irregular variations of the both annihilation characteristics

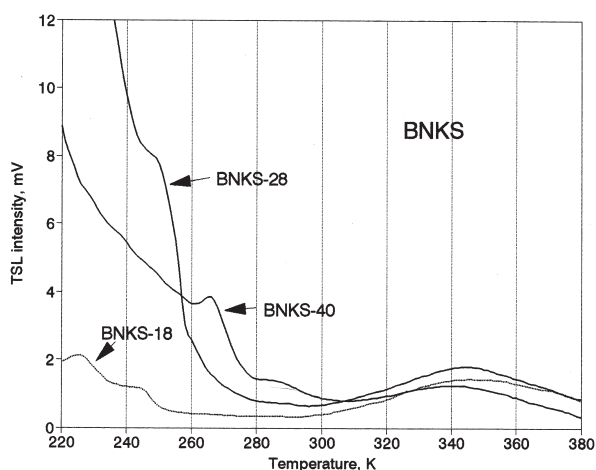


**Figure 19.** Results of TSL studies of BNKS. Integral intensity of TSL spectra as function of sample temperature. Typical example of  $T_g$  splitting (two peaks in the intensity curve) for BNKS(18%), compared to BNKS(28%) and BNKS(40%), illustrating in-homogeneity of BNKS(18%) structure.<sup>127</sup>

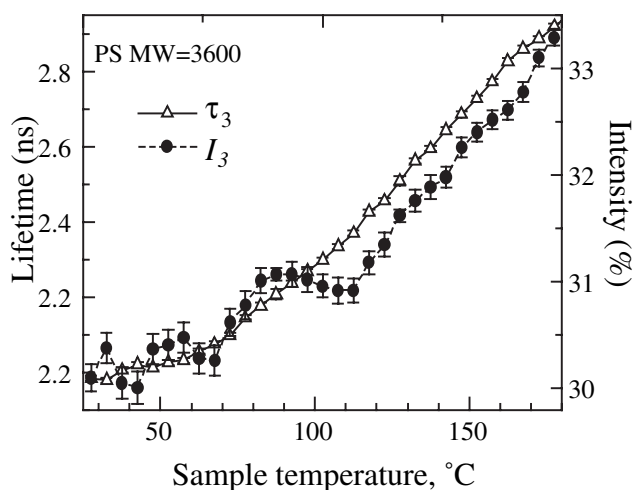


**Figure 20.** Variation of the positronium annihilation characteristics in polystyrene ( $MW=3.6 \times 10^3$ ,  $T_g=75$  °C) on heating from RT to 180 °C. Irregular (nonlinear, compare with Figure 8) variations of *o*-Ps intensity manifest structural transformations of the polymer above  $T_g$ .

( $\tau_3$  and  $I_3$ ) were found, so that glass transition temperature even could not be determined from positronium annihilation data. Obviously, this uncertainty infers inhomogeneity of the last polymer too. Both conclusions were confirmed using X-ray scattering.

**TFEMVE copolymer and poly(norbornen).** A dependence of the long positronium lifetime on temperature in the elastic copolymer of tetra-fluoro-ethylene and perfluoro-methyl-vinyl-ether (TFEMVE) (Figure 22) demonstrates smeared glass-transition (slow transformation of the structure) between  $-20$  and  $+60$  °C. Similarly, in metathesis poly (norbornen) of a composition 2-( $-\text{SiMe}_3$ )-PNB annihilation characteristics show complex variations of the structure between 50 and 170 °C (Figure 23) while listed  $T_g=167$  °C. We consider these results as an evidence of in-homogeneity of these two polymers too.

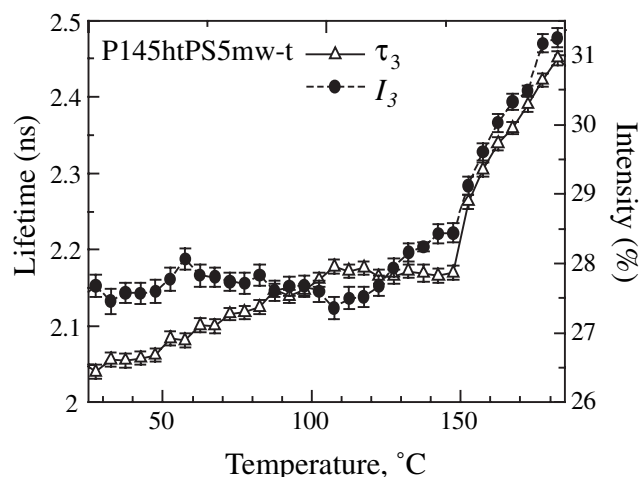


**Figure 21.** The same as in Figure 20, but for PS with  $MW=8 \times 10^5$ .<sup>127</sup>

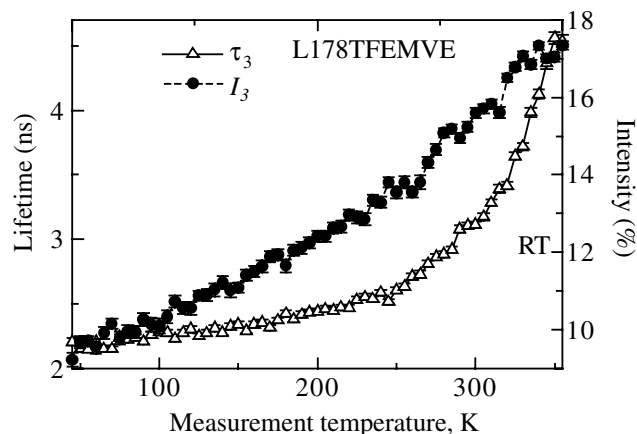


**Figure 22.** Temperature dependence of annihilation characteristics in TFEMVE.

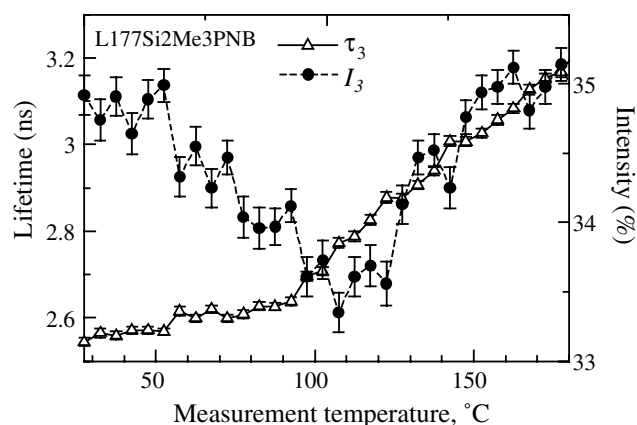


**Figure 23.** Temperature dependence of annihilation characteristics for 2-( $-\text{SiMe}_3$ )-PNB.<sup>127</sup>

**5.3. Relaxation effects in polymer glasses.** As we have seen from the previous section, PAL investigations show that many polymer glasses and rubbers may be inhomogeneous. This point of view is in agreement with one of the modern concepts of the glass structure, according to which amorphous polymers are characterized by long-lived fluctuations of density of a size about 300–2000 Å.<sup>128</sup> These fluctuations are responsible for super-slow  $\lambda$ -relaxation processes observed by dynamic mechanical spectroscopy technique above  $T_g$ . Figure 24<sup>128</sup> illustrates this point of view by the temperature dependence of internal friction, i.e. peaks on the curve of mechanical losses (logarithmic decrement  $\Delta$ ) at relaxation transition temperatures above  $T_g$ . Obviously, such situation infers slow relaxation of amorphous material, and such effects have to be seen in PAL measurements. In positron annihilation experiments, effects of thermal expansion (without structural transformations) are normally seen as linear (regular) variations of ortho-positronium annihilation characteristics (lifetime  $\tau_3$  and

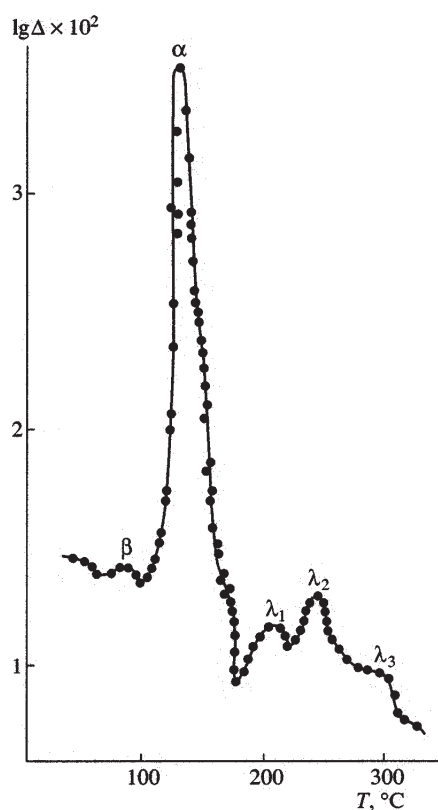


**Figure 24.** Spectrum of internal friction in PMMA (MW=5×10<sup>5</sup>,  $T_g$ =122 °C).  $\Delta$  is logarithmic decrement of mechanical losses.<sup>128</sup>

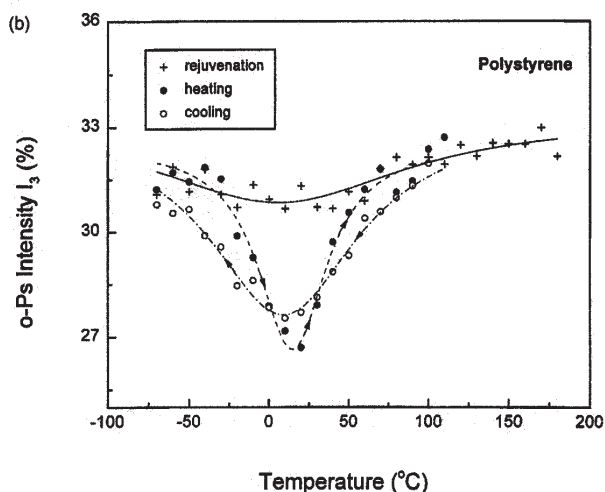


**Figure 25.** Temperature dependence of *o*-Ps lifetime  $\tau_3$  for polystyrene samples with different thermal treatment.<sup>129</sup>

intensity  $I_3$ ) and free volume parameters (see Figures 8 and 9). However, recent temperature-controlled experiments in polystyrene<sup>129</sup> revealed non-regular variations of these characteristics (minimum in variations of  $I_3$  at 220–340 K), showing structural changes (Figure 25). The variations could not be reproduced in full scale in the repeating cycles of measurements with the same sample kept for some time above glass transition temperature. Therefore such effects can be called “vanishing” effects<sup>130</sup> and are explained probably by slow relaxation processes in a polymer glass described above. Particularly, differential scanning calorimetry (DSC) measurements<sup>131</sup> demonstrated the role of intramolecular relaxation associated with mobility of phenyl groups ( $\beta$ -transition). Obtained results illustrate complex, dependent on thermal history, inhomogeneous character of the glass structure. In fact, structure of some polymer glasses is changing continuously.

## 6. Conclusion

On example of positron annihilation studies, we have got a glimpse of a quite interesting area of research, which came into being at the junction of several disciplines: elementary-particle physics, solid-state physics, and chemical kinetics. Referring to a number of examples we have seen how the employment of modern facilities of nuclear physics makes it possible, on the one hand, to identify a specific formation, one of the new atoms, called positronium, to study its transformations; on the other hand, to obtain valuable information about the structure and chemical properties of substances from the influence of the medium on the transformations of positronium. Analysis of intrinsic characteristics of positronium and bound states of positrons and comparison of these characteristics with predictions are also of great interest as a check on several model concepts and calculating techniques.<sup>132</sup>

We were not able to go into details of experimental arrangements, results of measurements and theoretical interpretations for other new atoms. This could be a topic of another review. It seems however that with section “introduction to new atoms” this paper is showing to a newcomer a little more than one of the specific applications of the positron annihilation method. In principle, the data on each of the new atoms and their comparison make physical information more complete and enable obtaining new interesting conclusions. The bibliography contains references to special reviews and original works to which the reader is referred for more profound treatments of the issues covered. We hope, it is seen from the review that studies of the physics and chemistry of the positronium at this stage not only made it possible to formulate the principal underlying concepts, but also resulted in a quite promising method of probing into physical and chemical properties of matter. And much of the information is either inaccessible with other methods or is obtained much simpler.

Beyond doubt, further development of experimental techniques and the joint efforts of physicists and chemists will expand these possibilities.

## References

- (1) B. A. Lambrecht, *Antimatter-Matter Interactions, Part 1*, BNL Rep. 50510, 1975.
- (2) J. Green and J. Lee, *Positronium Chemistry*, Academic Press, 1964.
- (3) V. I. Goldanskii, *Physical Chemistry of Positron and Positronium*, Moscow, Nauka, 1968 (in Russian).
- (4) Topics in Current Physics 12. *Positrons in Solids*, ed. P. Hautojarvi, Springer-Verlag, Berlin-Heidelberg, New York, 1979.
- (5) O. E. Mogensen, *Positron Annihilation in Chemistry*, Springer-Verlag, Berlin-Heidelberg, New York, 1995.

- (6) *Principles and Applications of Positron and Positronium Chemistry*. eds. Y. C. Jean, P. E. Mallon, and D. M. Schrader. World Scientific. New Jersey, London, Singapore, Hong-Kong, 2003.
- (7) V. I. Goldanskii and V. G. Firsov, *Ann. Rev. Phys. Chem.* **22**, 209 (1971).
- (8) J. A. Merrigan, J. H. Green, and S. J. Tao, *Physical Methods in Chemistry*, Part III D, eds. A. Weissberger and B. Rossiter, John Wiley and Sons (1972), p501.
- (9) H. J. Ache, *Angew. Chem. (Intern. Ed. )*, **11**, 179 (1972).
- (10) J. H. Green, *Radiochemistry*, ed. A. G. Maddock, London, Butterworth (1972), p251.
- (11) B. N. West, *Adv. Phys.* **22**, 263 (1973).
- (12) V. I. Goldanskii and V. P. Shantarovich, *Modern Physics in Chemistry*, Vol. 1, eds. E. Fluck and V. I. Goldanskii, London, Academic Press (1976), p269.
- (13) B. Levay, *At. Energ. Rev.* **17**, 413 (1979).
- (14) *Positron and Muon Chemistry*— Special Issue of *Radiation Physics and Chemistry*, ed. Y. Tabata, 1986.
- (15) J. Bartos, *Encyclopedia of Analytical Chemistry*. ed. R. A. Meyers, John Wiley & Sons, Chichester, 2000.
- (16) *Proc. 13th Int. Conf. Positron Annihilation (ICPA13)*, eds. T. Hyodo, Y. Kobayashi, Y. Nagashima, and M. Saito, Trans. Tech. Publications, 2004.
- (17) *8th Int. Workshop on Positron and Positronium Chemistry (PPC-8)*, 2005, to be published.
- (18) B. G. Hogg, G. M. Laidlaw, V. I. Goldanskii, and V. P. Shantarovich, *At. Energ. Rev.* **6**, 149 (1968).
- (19) B. M. Singru, K. B. Lal, and S. J. Tao, *At. Data Nucl. Data Tables*, **17**, 2725 (1976); **20**, 465 (1977).
- (20) V. P. Shantarovich, *J. Nuc. Radiochem. Sci.* **2**, R23 (2001).
- (21) V. P. Shantarovich, T. Suzuki, and C. He, *J. Radioanal. Nucl. Chem.* **255**, 165 (2003).
- (22) A. Ore, *Univ. Bergen Arb. Natur. Rekke*, **2**, 1 (1949).
- (23) V. A. Onishchuk and V. P. Shantarovich, *Khim. Vysok. Energ. (High Energy Chem. Russ.)* **14**, 472 (1980).
- (24) A. Foglio Para and E. Lazzarini, *J. Inorg. Nucl. Chem.* **42**, 475 (1980).
- (25) O. E. Mogensen, *J. Chem. Phys.* **60**, 998 (1974).
- (26) V. M. Byakov, V. I. Goldanskii, and V. P. Shantarovich, *Dokl. AN SSSR*, **219**, 633 (1974).
- (27) S. J. Tao, *Appl. Phys.* **3**, 1 (1974).
- (28) S. J. Tao, *Appl. Phys.* **10**, 67 (1976).
- (29) O. A. Anisimov and Yu. N. Molin, *Khim. Vysok. Energ. (High Energy Chem. Russ.)* **9**, 541 (1975).
- (30) V. M. Byakov, *Int. J. Radiat. Phys. Chem.* **8**, 283 (1976).
- (31) *Handbook of Radiochemistry*, eds. T. Tabata, Y. Ito, and S. Tagawa. CRC Press, Boca Raton, New York, 1991.
- (32) Y. Ito, *J. Radioanal. Nucl. Chem.* **210**, 327 (1996).
- (33) Y. Ito, *Mater. Sci. Forum* **255–257**, 104 (1997).
- (34) P. Jansen, M. Eldrup, S. B. Jansen, and O. E. Mogensen, *Chem. Phys.* **10**, 303 (1975).
- (35) M. Eldrup, V. P. Shantarovich, and O. E. Mogensen, *Chem. Phys.* **11**, 129 (1975).
- (36) A. G. Maddock, J. Ch. Abbe, and A. Haessler, *Chem. Phys.* **17**, 343 (1976).
- (37) A. G. Maddock, J. Ch. Abbe, and A. Haessler, *Chem. Phys. Lett.* **47**, 314 (1977).
- (38) G. Duplatre, A. G. Maddock, J. Ch. Abbe, and A. Haessler, *Chem. Phys.* **28**, 433 (1978).
- (39) V. L. Bugaenko, V. M. Byakov, and V. I. Grafutin, *Radiat. Phys. Chem.* **11**, 145 (1978).
- (40) V. M. Byakov, V. I. Grafutin, O. V. Koldaeva, and E. V. Minaichev, *Radiochem. Radioanal. Lett.* **54**, 283 (1982).
- (41) A. Bisi, G. Gambarini, and L. Zappa, *Lett. Nuovo Cim.* **31**, 58 (1981).
- (42) W. Brandt, *Lett. Nuovo Cim.* **33**, 409 (1982).
- (43) O. E. Mogeusen, *Phys. Lett. A*, **96A**, 250 (1983).
- (44) L. G. Aravin, V. I. Goldanskii, V. P. Shantarovich, and M. K. Filimonov, *Khim. Vysok. Energ. (High Energy Chem. Russ.)* **3**, 1287 (1984).
- (45) V. P. Shantarovich, T. Hirade, I. B. Kevdina, V. W. Gustov, and E. F. Oleinik, *Acta Phys. Pol.* **A99**, 497 (2001).
- (46) V. A. Onishchuk and V. P. Shantarovich, *Khim. Vysok. Energ. (High Energy Chem. Russ.)* **16**, 360 (1982).
- (47) J. Dezsai, Zs. Kajcsos, and B. Molnar, *Nucl. Instrum. Methods.* **141**, 401 (1977).
- (48) Y. C. Jean, P. E. Mallon, R. Zhang, H. Chen, and Y. C. Wu, see Ref. 6, p221.
- (49) M. Eldrup, V. P. Shantarovich, and O. E. Mogensen, *Chem. Phys.* **11**, 129 (1975).
- (50) V. I. Goldanskii, A. O. Tatur, V. P. Shantarovich, and A. V. Shishkin, *Dokl. AN SSSR*, **229**, 80 (1976).
- (51) V. I. Goldanskii, V. P. Shantarovich, and A. V. Shishkin, *Khim. Vysok. Energ. (High Energy Chem. Russ.)*, **2**, 179 (1977).
- (52) V. I. Goldanskii, K. Petersen, V. P. Shantarovich, and A. V. Shishkin, *Appl. Phys.* **16**, 413 (1978).
- (53) P. A. Kumar, M. Alotalo, V. J. Ghosh, A. C. Kruseman, B. Nielsen, and K. G. Lynn, *Phys. Rev. Lett.* **77**, 2097 (1996).
- (54) Y. Ito and T. Suzuki, *Rad. Phys. Chem.* **58**, 743 (2000).
- (55) V. P. Shantarovich, T. Suzuki, C. He, and V. W. Gustov, *Rad. Phys. Chem.* **67**, 15 (2003).
- (56) B. A. Ferrell, *Phys. Rev.* **108**, 167 (1957).
- (57) L. O. Roellig, *Positron Annihilation*, eds. A. T. Stewart and L. O. Roellig, Academic Press (1967), p127.
- (58) P. Hautojarvi, M. T. Loponen, and K. Rytola, *Phys. B*, **9**, 411 (1976).
- (59) A. P. Buchikhin, V. I. Goldanskii, and V. P. Shantarovich, *Pis'ma Zhurn. Eksp. Teor. Fiz.* **13**, 624 (1971).
- (60) A. P. Buchikhin, V. I. Goldanskii, A. O. Tatur, and V. P. Shantarovich, *Zhurn. Eksp. Teor. Fiz.* **60**, 1136 (1971).
- (61) S. J. Tao, *J. Chem. Phys.* **56**, 5499 (1972).
- (62) B. Levay, A. Vertes, and P. Hautojarvi, *J. Phys. Chem.* **77**, 2229 (1973).
- (63) F. A. Smith and C. D. Beling, *Chem. Phys.* **55**, 177 (1981).
- (64) V. M. Byakov and V. R. Petukhov, *Radiochem. Radioanal. Lett.* **58**, 91 (1983).
- (65) P. R. Gray, C. F. Cook, and G. F. Sturm, *J. Chem. Phys.* **48**, 1145 (1968).
- (66) V. I. Goldanskii, I. B. Kevdina, and V. P. Shantarovich, *Izv. AN SSSR, Ser. Khim.* **3**, 683 (1975).
- (67) A. P. Buchikhin, V. I. Goldanskii, and V. P. Shantarovich, *Dokl. Akad. Nauk SSSR* **212**, 1356 (1973).
- (68) V. I. Goldanskii and V. P. Shantarovich, *Appl. Phys.* **3**, 353 (1974).
- (69) W. Brandt and J. Spirn, *Phys. Rev.* **142**, 231 (1966).
- (70) V. P. Shantarovich and P. Jensen, *Chem. Phys.* **34**, 39 (1978).
- (71) K. V. Mikhin, S. V. Stepanov, and V. M. Byakov, *Khim. Vys. Energ. (High Energy Chem. Russ.)*, **39**, 44 (2005).
- (72) R. S. Yu, T. Suzuki, Y. Ito, N. Djourelou, K. Kondo, and V. P. Shantarovich, *Chem. Phys. Lett.* **406**, 101 (2005).
- (73) J. Bartos, O. Sausa, P. Bandzuch, J. Zrubkova, and J. Kristiak, *J. Non-Crystalline Solids* **307–310**, 417 (2002).
- (74) W. Brandt and R. Paulin, *Phys. Rev.* **B6**, 2430 (1972).
- (75) W. Brandt, *Appl. Phys.* **5**, 1 (1974).
- (76) A. E. Hamielec, M. Eldrup, O. Mogensen, and P. Jansen, *J. Macromol. Sci.* **C9**, 305 (1973).
- (77) J. R. Stevens and M. J. Edwards, *J. Polym. Sci. C* **30**, 397 (1970); *Kautsch.* **29**, 271 (1982).
- (78) V. A. Onishchuk, V. S. Pudov, V. P. Shantarovich, and L. L. Yasina, *Vysokomolek. Soedin.* **12**, 2579 (1982).
- (79) O. G. Alexanyan, A. A. Berlin, A. V. Goldanskii, N. S. Grineva, V. A. Onishchuk, V. P. Shantarovich, and G. P. Safonov, *Khim. Fiz. (Chem. Phys. Russ.)*, **5**, 1225 (1986).
- (80) V. V. Volkov, A. V. Goldanskii, F. G. Durgar'yan, V. A. Onishchuk, V. P. Shantarovich, and Yu. P. Yampolskii,

- Vyzokomolek. Soedin. (Polymer Science, Russ.), A **1**, 198 (1987).
- (82) A. V. Goldanskii, V. A. Onishchuk, V. P. Shantarovich, M. S. Akutin, N. B. Enikolopova, and E. D. Lebedeva, *Dokl. AN SSSR*, **298**, 633 (1988).
- (83) P. Kirkegaard and M. Eldrup, *Comp. Phys. Commun.* **7**, 401 (1974).
- (84) M. Eldrup, D. Lightbody, and J. N. Sherwood, *Chem. Phys.* **63**, 51 (1981).
- (85) Q. Deng and Y. C. Jean, *Macromolecules* **26**, 30 (1993).
- (86) Q. Deng, F. Zandiehnam, and Y. C. Jean, *Macromolecules* **25**, 1090 (1992).
- (87) V. P. Shantarovich, T. Suzuki, N. Djorelov, A. Shimazu, V. W. Gustov, and I. B. Kevdina, *Acta Phys. Pol. A* **107**, 629 (2005).
- (88) V. P. Shantarovich, T. Suzuki, C. He, V. A. Davankov, A. V. Pastukhov, M. P. Tsyurupa, K. Kondo, and Y. Ito, *Macromolecules* **35**, 9723 (2002).
- (89) S. J. Gregg and K. S. W. Sing, *Absorption, Surface and Porosity, 2nd ed.* Academic Press, London, 1984.
- (90) T. Goworek, K. Ciesielski, B. Jasinska, and J. Wawryszczuk, *Chem. Phys.* **230**, 305 (1998).
- (91) B. Jasinska, A. E. Koziel, and T. Goworek, *J. Radioanal. Nucl. Chem.* **210**, 617 (1996).
- (92) D. W. Gidley, W. Frieze, T. L. Dull, A. F. Yee, E. T. Ryan, and H. M. Ho, *Phys. Rev. B* **60**, 5157 (1999).
- (93) T. L. Dull, W. E. Frieze, D. W. Gidley, J. N. Sun, and A. F. Yee, *J. Phys. Chem. B* **105**, 4657 (2001).
- (94) C. He, T. Suzuki, V. P. Shantarovich, K. Kondo, and Y. Ito, *Chem. Phys.* **286**, 249 (2003).
- (95) N. Djourelov, T. Suzuki, V. P. Shantarovich, and K. Kondo, *Radiat. Phys. Chem.* **72**, 723 (2005).
- (96) V. P. Shantarovich, T. Suzuki, C. He, N. Djourelov, I. B. Kevdina, V. A. Davankov, A. V. Pastukhov, and Y. Ito, *Mater. Sci. Forum* **445–446**, 346 (2004).
- (97) J. Kansy and T. Suzuki, *Radiat. Phys. Chem.* **68**, 497 (2003).
- (98) S. V. Stepanov and V. M. Byakov, *Principles and Applications of Positron and Positronium Chemistry*, eds. Y. C. Jean, P. E. Mallon, and D. M. Schrader, World Scientific (2003), p117.
- (99) C. Dauwe, B. van Waeyenberge, and J. de Baerdemaeker, *Mater. Sci. Forum* **445–446**, 229 (2004).
- (100) T. Hirade, F. H. J. Maurer, and M. E. Eldrup, *Radiat. Phys. Chem.* **58**, 465 (2000).
- (101) K. W. Waran, K. L. Cheng, and Y. C. Jean, *J. Phys. Chem.* **88**, 2465 (1984).
- (102) V. P. Shantarovich and V. I. Goldanskii, *Hyperfine Interact.* **116**, 67 (1998).
- (103) V. P. Shantarovich, Z. K. Azamatova, A. Yu. Novikov, and Yu. P. Yampolskii, *Macromolecules* **31**, 3963 (1998).
- (104) V. P. Shantarovich, Yu. P. Yampolskii, Yu. M. Sivergin, O. B. Salamatina, V. W. Gustov, and D. Hofmann, *Khimicheskaya Fizika (Chemical Physics, Russ.)*, **22**, 87 (2003).
- (105) K. Hirata, Y. Kobayashi, and Y. Ujihira, *J. Chem. Soc. Faraday Trans.* **92**, 985 (1996).
- (106) G. Dlubek, K. Saarinen, and H. M. Fretwell, *Polymer Science, Part B*, **36**, 1513 (1998).
- (107) J. Kristiak, P. Bandzuch, P. Sausa, J. Zrubkova, and J. Bartosh, *Mater. Sci. Forum* **363–365**, 269 (2001).
- (108) H. A. Hristov, B. Bolan, A. F. Ye, L. Xie, and D. W. Gidley, *Macromolecules* **29**, 8507 (1996).
- (109) R. F. Boyer and R. Simha, *J. Polym. Sci. (Polymer Letters Edition) B* **11**, 33 (1973).
- (110) G. Dlubek, V. Bondarenko, J. Piontek, M. Supej, A. Wutzler, and R. Krauze-Rehberg, *Polymer*, **44**, 1921 (2003).
- (111) V. P. Shantarovich, T. Suzuki, C. He, Y. Ito, Yu. P. Yampolskii, and A. Yu. Alentiev, *Radiat. Phys. Chem.* **73**, 45 (2005).
- (112) T. Suzuki, Y. Oki, M. Numajiri, T. Miura, K. Kondo, N. Oshima, and Y. Ito, *Polymer* **37**, 5521 (1996).
- (113) T. Hirade, C. L. Wang, F. H. J. Maurer, M. Eldrup, and N. J. Pedersen, *Abstract book for the 35th Annual meeting on radioisotopes in physical science and industries*, Tokyo (1998), p89.
- (114) T. Hirade, F. H. J. Maurer, and M. Eldrup, *Radiat. Phys. Chem.* **58**, 465 (2000).
- (115) T. Hirade, *Mater. Sci. Forum* **445–446**, 234 (2004).
- (116) V. P. Shantarovich, T. Hirade, I. B. Kevdina, V. W. Gustov, and M. S. Arzhakov, *Mater. Sci. Forum* **363–365**, 352 (2001).
- (117) C. He, V. P. Shantarovich, T. Suzuki, S. V. Stepanov, R. Suzuki, and M. Matsuo, *J. Chem. Phys.* **122**, 214907 (2005).
- (118) R. S. Brusa, M. Duarte Naia, D. Margoni, and A. Zecca, *Appl. Phys. A* **60**, 447 (1995).
- (119) C. Dauwe, B. Van Waeyenberge, and N. Balcaen, *Phys. Rev. B* **68**, 132202 (2003).
- (120) T. Goworek, T. Suzuki, E. Hamada, K. Kondo, and Y. Ito, *Chem. Phys.* **255**, 347 (2000).
- (121) T. Goworek, *Mater. Sci. Forum* **363–365**, 227 (2001).
- (122) V. P. Shantarovich, T. Suzuki, R. S. Yu, K. Kondo, V. W. Gustov, I. V. Melikhov, S. S. Berdonosov, and L. N. Ivanov, *Proc. 8th Int. Workshop on Positron and Positronium Chemistry (PPC-8)*, rep. I6. 3, 2005.
- (123) D. V. Krevelen and P. J. van Hoftyzer, *Properties of Polymers. Their Estimation and Correlation with Chemical Structure*. Elsevier, Amsterdam, Oxford, New York (1976), p126.
- (124) G. Dlubek, S. Eichler, Ch. Hubner, and Ch. Nagel, *Phys. Stat. Sol. (a)* **174**, 313 (1999).
- (125) G. Dlubek and S. Eichler, *Phys. Stat. Sol. (a)* **168**, 333 (1998).
- (126) C. He, T. Suzuki, V. P. Shantarovich, K. Kondo, and Y. Ito, *Chem. Phys.* **286**, 249 (2003).
- (127) V. P. Shantarovich, T. Suzuki, Y. Ito, K. Kondo, V. W. Gustov, A. V. Pastukhov, L. V. Sokolova, A. V. Polyakova, E. V. Belousova, and Yu. P. Yampolskii, *J. Radioanal. Nucl. Chem. in press*.
- (128) G. M. Bartenev and V. A. Lomovskoy, *Vysokomolekulyarnye Soedineniya (Russ. Macromolecules)* **44**, 1331 (2002).
- (129) Z. L. Peng, B. G. Olson, J. D. McGervey, and A. M. Jamieson, *Polymer* **40**, 3033 (1999).
- (130) V. P. Shantarovich, T. Suzuki, Y. Ito, R. S. Yu, K. Kondo, Yu. P. Yampolskii, and A. Yu. Alentiev, *Proc. 8th Int. Workshop on Positron and Positronium Chemistry*, Coimbra, Portugal, Rep. PS8, 2005.
- (131) N. Bach Van and C. Noel, *J. Polym. Sci.* **16**, 1627 (1976).
- (132) A. Rich, *Modern Phys.* **53**, 127 (1981)